COMPLEX VELOCITY MODEL BUILDING OF FIMKASSAR AREA, UPPER INDUS BASIN, PAKISTAN

MUHAMMAD MUNEEB

01-262192-025

A thesis submitted in Fulfilment of the

Requirements for the award of the degree of

Master's in science (Geophysics)

Department of Earth and environmental Science

Bahria University Islamabad

2021

THESIS COMPLETION CERTIFICATE

Scholar's Name: Muhammad Muneeb Registration No. 42150

Program of study: MS (Geophysics)

Thesis Title: Complex velocity model building of Fimkassar area, Upper Indus Basin Pakistan.

It is to certify that the above student's thesis has been completed to my satisfaction and, to my belief, its standard is appropriate for submission for Evaluation. I have also conducted plagiarism test of this thesis using HEC prescribed software and found similarity index at **6%** that is within the permissible limit set by the HEC for the MS/MPhil degree thesis. I have also found the thesis in a format recognized by the BU for the MS/MPhil thesis.

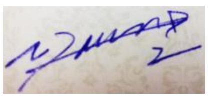

Principal Supervisor's Signature:

____

Date: 08/09/2021 **Name: Dr. Muhammad Fahad Mahmood**

AUTHOR'S DECLARATION

I, Muhammad Muneeb hereby state that my MS thesis titled "Complex velocity model building of Fimkassar area, Upper Indus Basin Pakistan." is my own work and has not been submitted previously by me for taking any degree from this university (Bahria University Islamabad Campus) or anywhere else in the country/world.

At any time if my statement is found to be incorrect even after my graduation, the University has the right to withdraw/cancel my MS degree.

Name of scholar: Muhammad Muneeb

Date: 08/09/2021

PLAGIARISM UNDERTAKING

I, solemnly declare that research work presented in the thesis titled "Complex velocity model building of Fimkassar area, Upper Indus Basin Pakistan." is solely my research work with no significant contribution from any other person. Small contribution / help wherever taken has been duly acknowledged and that complete thesis has been written by me.

I understand the zero-tolerance policy of the HEC and Bahria University towards plagiarism. Therefore, I as an Author of the above titled thesis declare that no portion of my thesis has been plagiarized and any material used as reference is properly referred / cited.

I undertake that if I am found guilty of any formal plagiarism in the above titled thesis even after award of MS degree, the university reserves the right to withdraw / revoke my MS degree and that HEC and the University has the right to publish my name on the HEC / University website on which names of scholars are placed who submitted plagiarized thesis.

Scholar / Author's Sign

Name of the Scholar: Muhammad Muneeb

ACKNOWLEDGEMENTS

Prima facia, I am grateful to Almighty Allah the most cordial and sympathy who's blessing always enabled us to perceive and pursue most difficult target of life. All respects are for the Holy Prophet Hazrat Mohammad (S.A.W) who is forever a beacon of guidance and knowledge for humanity as a whole and enable us to recognize our creator. He is forever a model of guidance and knowledge for the whole mankind.

I wish to express my sincere thanks to Dr. Fahad Mahmood, my supervisor, for providing me with all the necessary facilities for the research.

I place on record, my sincere thanks to Dr. Khalid Amin Khan Oil & Gas Development Company Ltd, for his continuous support. His help and direction provided me a framework that aided the progress towards my goal, I am extremely thankful and indebted to him for sharing expertise, and sincere and valuable guidance and encouragement extended to me.

I take this opportunity to express gratitude to all the Department faculty members for their help and support. I also thank my parents for the unceasing encouragement, support, and attention. I also place on record, my sense of gratitude to one and all, who directly or indirectly, have lent their hand in this journey

ABSTRACT

The present study was accompanied to delineate the subsurface geology of Fimkassar area by the structural interpretation of seismic. The Fimkassar area lies within the Upper Indus Basin in SE of Salt range Potwar Foreland Basin. The marked horizons are recognized using Formation tops from wells Turkwal-01 and Turkwal Deep-01. Seismic interpretation of the given 2D Information reveals that the study area has undergone severe distortion illustrated by the event of thrusts and back thrusts forming a triangle zone within the subsurface showing a pop-up geometry. The zones interpreted by the study includes Khewra Sandstone and Chorgali Formation that could have the most important crude potential within the study area.

Velocity modelling was carried out on all seismic data which gave more accurate interpolated velocity according to geological cross section of area. The interpolated velocity was then used in post stack depth and time migration. The migrated section gave more clear sections with reduced noise and clearer picture of subsurface i.e., faults and horizons were more visible.

TABLE OF CONTENTS

LIST OF TABLES

LIST OF FIGURES

CHAPTER 1

INTRODUCTION

1.1 INTRODUCTION TO STUDY AREA

Fimkassar formerly named Parhal field is in Southern Potwar on OGDCL's Fimkassar concession in Punjab's Chakwal district Pakistan. The study area is Fim Kassar located between latitude 33.01343-32.9817 and longitude 72.8472-72.8012 which is situated above sea level 494 meters. Study area is in Chakwal District of Punjab region tectonically located in Potwar sub-basin of Upper Indus Basin Pakistan. Fimkassar is 72 km South of Islamabad.

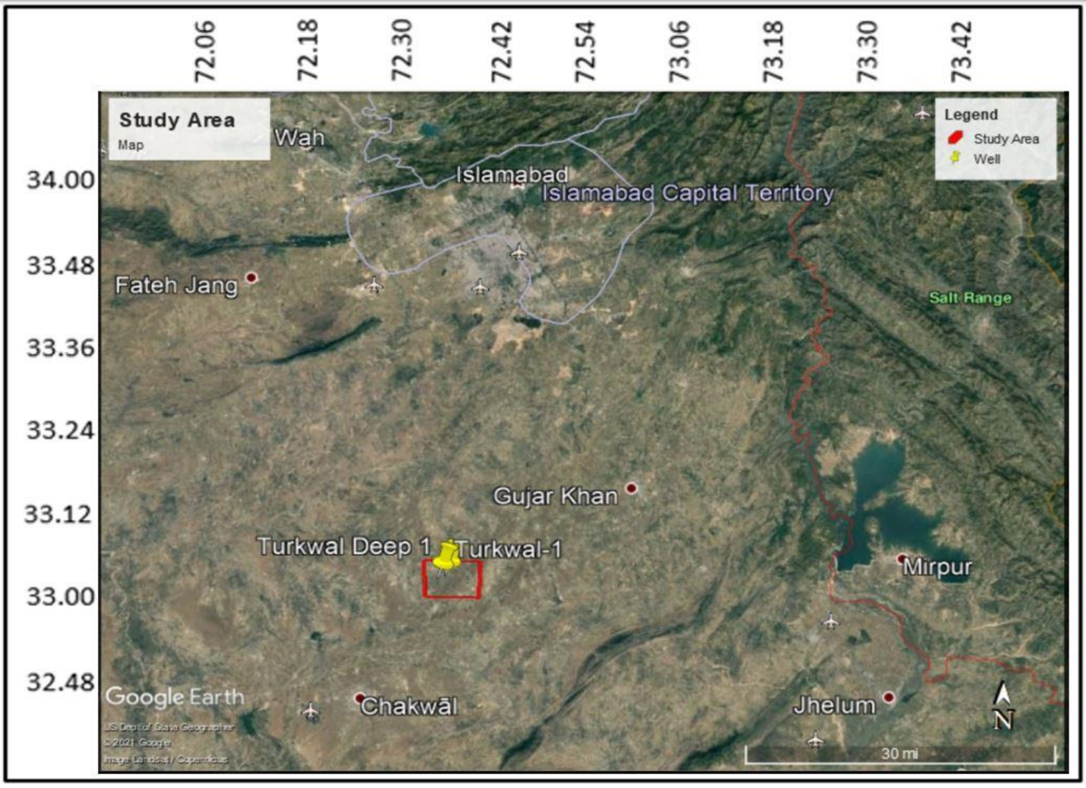

Figure 1.1 Location of the study area (Google Earth)

1.2 GENERAL INTRODUCTION

The Potwar Sub-basin is in the western foothills of the Himalayas on the northern margin of Pakistan. It comprises the Potwar Plateau, the Jhelum Plain, and Salt Range. From the main thrust belt to the north, towards south Salt Range, towards west the Indus and Kalabagh faults, and the Jhelum strike slip faults to the east, the total length is approximately 130 kilometers. The Potwar sub-basin is full of thick Precambrian evaporites, enclosed with relatively thin platform sediments from Cambrian to Eocene, followed by thick molasses of Miocene-Pliocene. The entire section was sternly distorted by the extremely strong Himalayan orogenic movement that occurred from the Pliocene to the Middle Pleistocene.

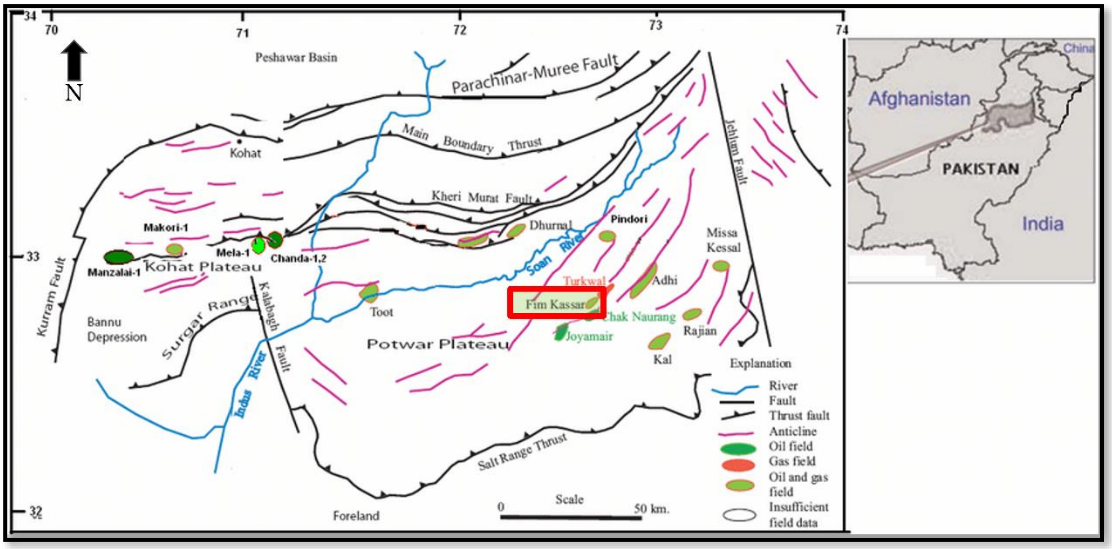

Figure 1.2 Geological Location of study area (Kazmi and Rana, 1982)

The average height of the area is 500 m to 550 m. The Punjab Plain in Kalabagh is drained by the Indus River and the Soan River. So far around 150 exploration wells have been drilled in the area, but due to the complex structure, there is high pressure water in the Mollasse deposit, the wells cannot reach the target depth, so many wells were abandoned. The framework and structural style of the basin can be provided by underground images (Yeats et al., 1984).

The Fimkassar, Chak Naurang, Joyamir, Adhi and Balkassar oil fields use Sakesar and Chorgali Formations as reservoirs, while the Rajian, Adhi and Chak-Naurang oil fields use the Khewra sandstone as reservoirs.

The area is a system of residual knolls and hills that are formed from glacial debris as remnants of the ice age and comprises mostly on sedimentary rocks of tertiary origin. Its height varies from 1000 to 2000 feet.

1.3 FIMKASSAR OILFIELD

Fimkassar Oilfield which was first known as Parhal field is situated in the Southerrn Potwar region which is the concession of OGDCL's Punjab region in Chakwal District of Pakistan. The structure of Fimkassar is located at South-Eastern part of Potwar Basin and has a trend of 23 by 13 m North-East, South-West, surface expression with vertical closure of 1800-1900 m. Fimkassar 01 oil discovery was declared by Gulf oil in June 1981. Chorgali Formation present at the depth of 2891-3081m which produces oil for the well. Total depth was 2,730 m (hole A), 2253 m (sidetrack hole A), 7081m (hole B), 2360 (side hole B). Original reserves were 30 million bbl., and 1994 production was 2562 bbl. of oil.

Geographically Fimkassar Field is situated 72 km southwest of Islamabad. Initially the drilling in the field started in 1981 when Texas Gulf drilled Fimkassar X1. Later on, OGDCL takeover the field and resume the drilling of well and abandon the well. Till date five wells have been drilled on Fimkassar structure.

1.4 CLIMATE

The weather of the region is moderate, it is hot in summers and mostly cold/dry in winter. The temperature in summer season rises to 38° centigrade and in winter temperature falls to 4° centigrade. The recorded average rainfall in the area is 10.1mm. The yearly picture (fig 1.3) is showing results on data collected from 1985 to 2018.

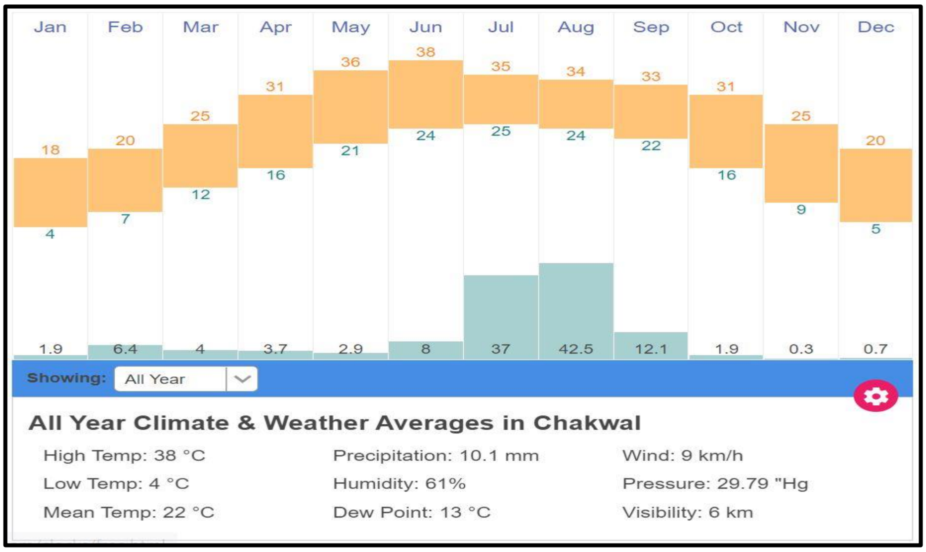

Figure 1.3 Average annual temperature of study area, Potwar basin, Pakistan. (en.climate-data.org)

1.5 AVAILABLE DATA

The objective of the research work is to comprehend the different steps which are involved in seismic interpretation and correlate the seismic data with the results obtained from the well data to generate a structural model of the study area. For thesis work, the Directorate General of Petroleum Concessions Pakistan provided seismic reflection data, including seven Seismic lines and two well data, at the application of the head of the Department of Earth and Environmental Sciences at the Bahria University in Islamabad.

1.5.1 Seismic lines

The following seismic lines were used for thesis work.

1 884-FMK-03 (Dip line)
2 884-FMK-04 (Strike line)
3 884-FMK-06 (Strike line)
4 884-FMK-07 (Dip line)
5 884-FMK-08 (Dip line)
6 96-PW-03 (Dip line)

1.5.2 Well data

The following wells were used for thesis work.

1 Turkwal-1
2 Turkwal Deep-1

1.5.3 Base map

The map in figure 1.4 shows the display of six seismic lines in which two lines are strike lines and five are dip lines. Two wells are also displayed on the base map of Fimkassar area.

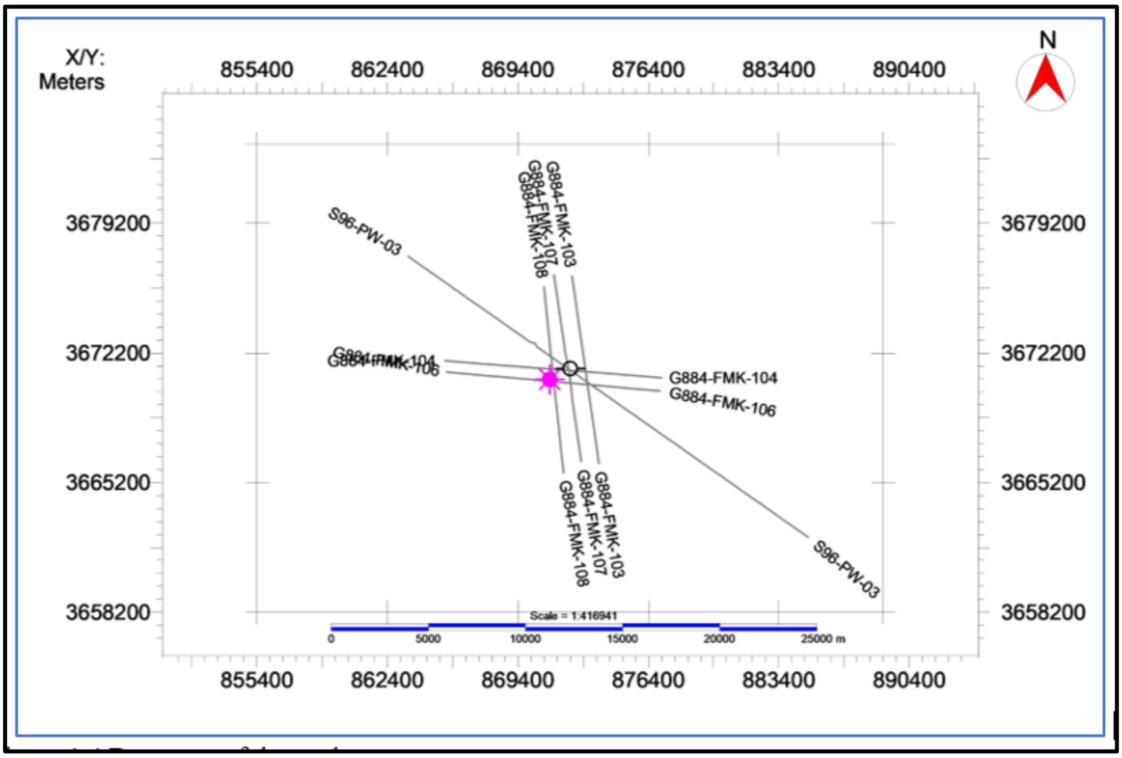

Figure 1.4 Base map of the study area.

1.6 OBJECTIVE OF RESEARCH

The main objective of this thesis is lined up as follows:

1. Carry out seismic interpretation and mapping of the area to understand the subsurface trends.
2. Perform velocity modeling and develop understanding of geological complexity of area.
3. To make depth maps using the modeled velocity for finding true depth of reservoir zone.
4. Carry out post-Stack depth migration using velocity models for true interpretation.

1.7 METHODOLOGY

The methods used to achieve the research objectives are as follows:

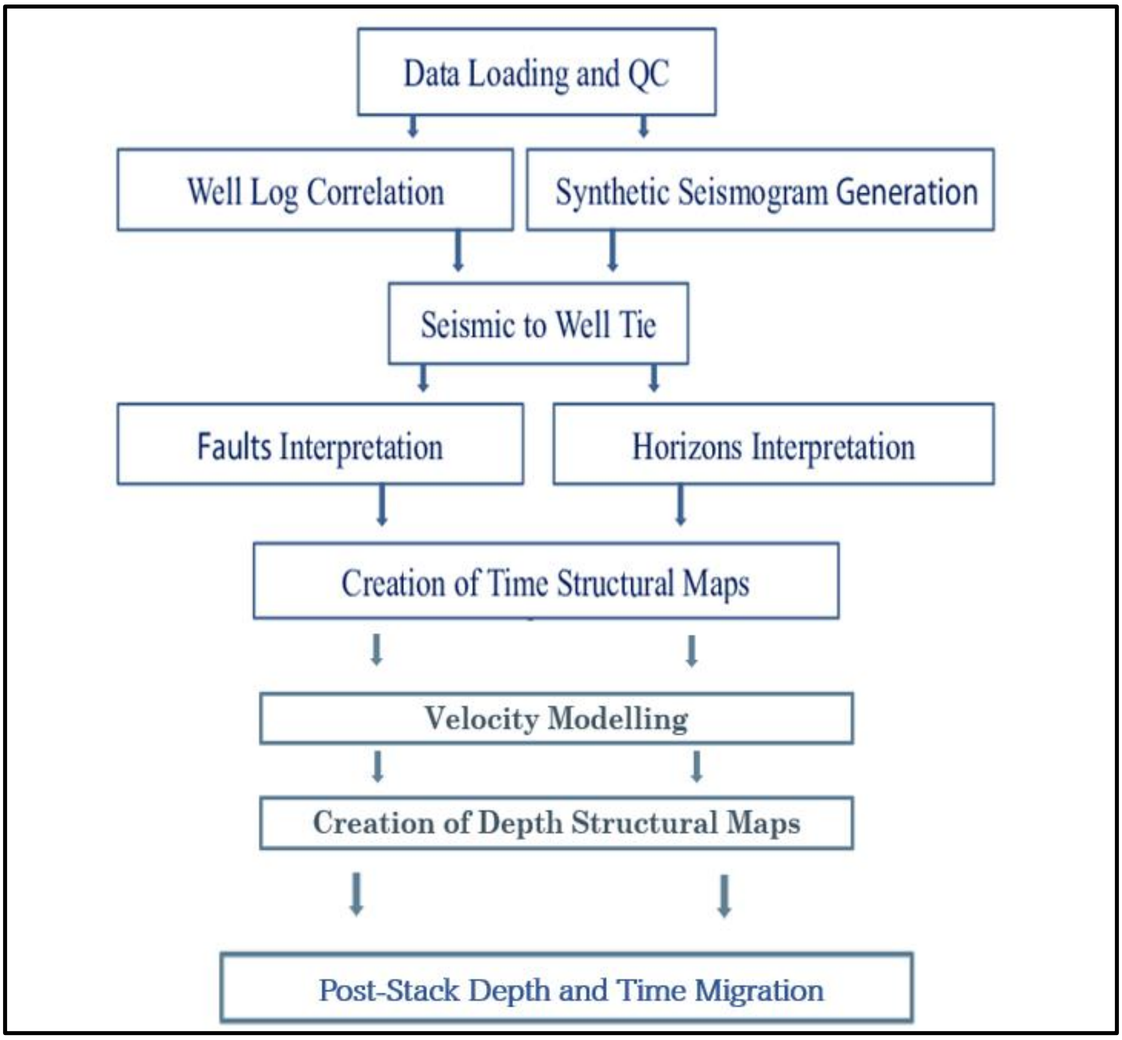

Figure 1.5 Flowchart showing methodology of thesis work.

CHAPTER 2

GEOLOGICAL AND TECTONIC SETTING AND PETROLEUM PLAY OF STUDY AREA

2.1 GENERAL GEOLOGY

The Fimkassar area and part of the Adhi structure in the Potwar sedimentary basin. The stratigraphic units have been well identified and the geology has been studied extensively. The fault propagation fold is the structure of the Pliocene-Pleistocene era and is striking in NE-SW (Moghal et al., 2007).

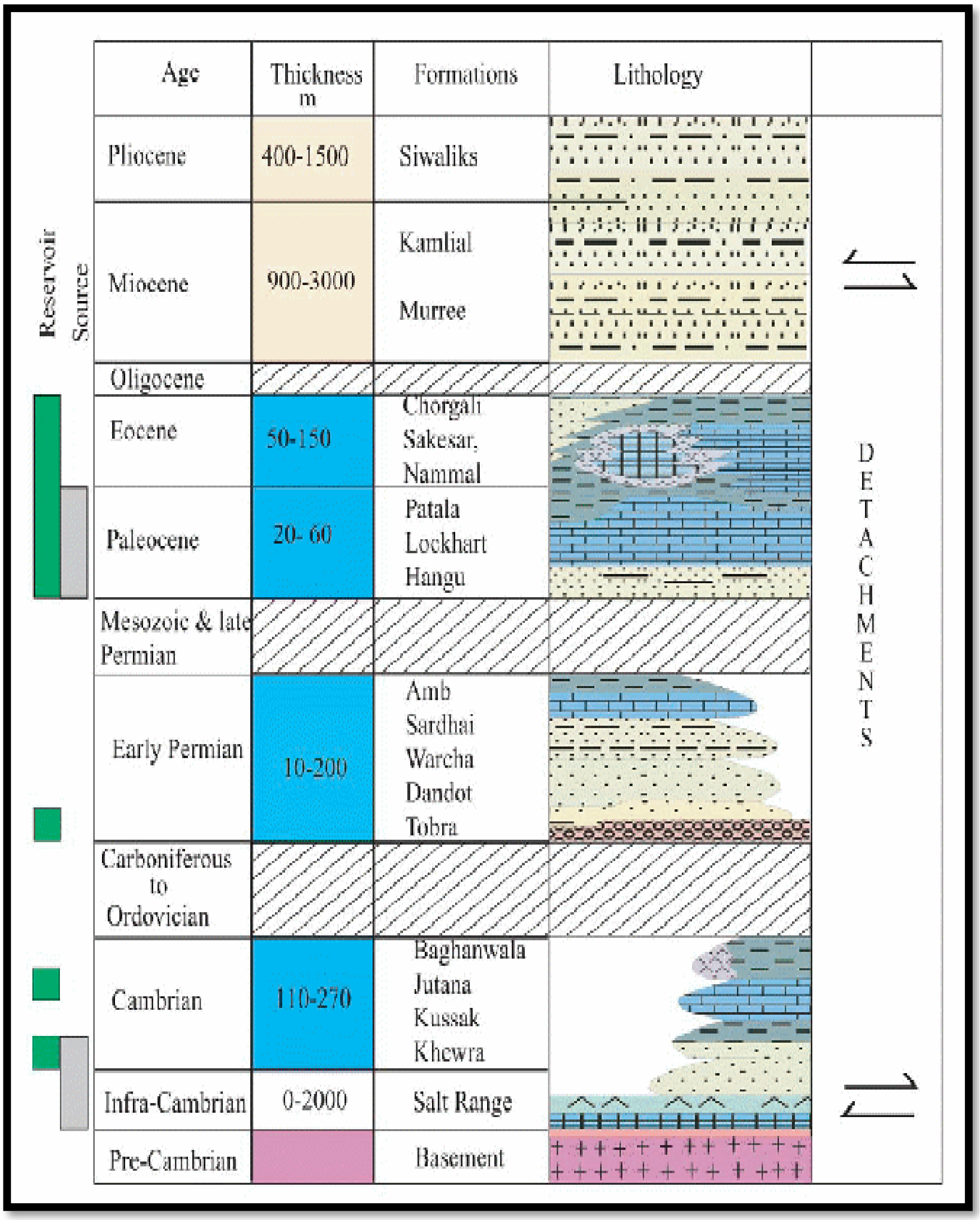

Figure 2.1 Stratigraphic map and petroleum play of the Upper Indus Basin. (Qadri, 1995)

This structure is believed to be rich in potential hydrocarbons and slopes upward from the Soan depression in the northwest. It is part of a large structure bounded by 1800 milliseconds (TWT) and overlapping thrust faults (Moghal et al., 2007).

A trough of molasses sediments of Neogene age is formed by Potwar basin, and it is related to the Himalayan orangey of Tertiary era. The molasse sediments overlie a brain, basal sequence of caline series acted as decollement layer between Pre-Cambrian basement and overlaying sediments (post-Cambrian) and resulted in structural Deformation.

2.2 PRECAMBRIAN ROCKS

In the basement rocks of Himalayas salt range Formation and possibly in the Karakorum Range, Precambrian sedimentary and meta-sedimentary rocks are exposed. The closure of the Neo-tethys Ocean commenced the Eocene Oligocene uplift related to Himalayan collision. The SRPFB was commenced by the Himalayan collision, which was accumulated by a thick sandstone-clay cyclic molassess sequences. Murree, Kamlial, Chinji, Nagri, Dhok pathan and Soan Formations are comprised by the Miocene to Pleistocene molasses deposits (Shah, 2009).

In the north the erosion product of the uplifting Himalayan foreland fold and thrust belts is characterized by the time transgressed molasses deposits. The total thickness of Molasse sequence is 5500 meters in SRPFB (Moghal et al., 2007).

2.3 BASEMENT ROCKS

The oldest rocks of Pakistan firstly belong to the Pre-Cambrian age, secondly, they form the basement for the lower Paleozoic sediments, and thirdly it serves as the source of terrigenous clastics for the younger rocks in adjoining areas.

2.4 SALT RANGE FORMATION

There are three members of Salt Range Formation which are Billianwala Salt member, Bandar Khas Gypsum and Sahwal Marl member. Billianwala Salt member comprises hematitic and dim red gypsiferous marly beds, have thick seams of salt. Bandar Khas Gypsum includes massive marl, gypsum and dolomite. Sahwal Marl member represent upper bright marly unit contains dim red marl (Shah, 2009).

2.4.1 Sahwal marl member

Here red marl beds containing salt seams of salt and on the top gypsum bed which is approximately 10meters thick (more than 40meters). Also found here are perky red marl beds with irregular gypsum, beds of dolomite and khewra trap (3-100meters).

2.4.2 Bandar Kas Gypsum member

The Bandar Kas Gypsum is a massive gypsum group, which contains minor beds of dolomite and clay (more than 80 meters).

2.4.3 Billanwala salt member

Here ferriginous red marl with thick seams of salt can be found (more than 650 meters).

2.5 DECOLLEMENT

Salt range Formation act as a decollement between platform sequence on the top and basement underlying it and it is one of its most important features (Moghal et al, 2007).

2.6 CAMBRIAN

Jhelum group is the name given to the Rocks of Cambrian age collectively. These are comprehensively found along the southern boundary of Kohat Potwar basin forming accurate beds. Several wells indicated the presence of Khewra Formation in the sub-surface in the Potwar basin. These sediments are thought to underlie Karampur well. Cambrain sediments are considered to occupy a total area of about 25000sq kilometers based on surface and subsurface evidence (Moghal et al., 2007).

2.6.1 Khewra Sandstone

The Formation represent sandstone with minor claystone. Sandstone is of purple to light brown color, fine to medium grained, mostly sorted and are argillaceous. Claystone are of light brown to brick red, fissile and non-calcareous. The depositional environment is shallow marine, littoral to sublittoral. The age of this Formation is Cambrian (Shah, 2009).

2.7 PERMIAN

In Upper Indus Basin Permian strata have been further divided into Nilawahan group and Zaluch group

2.7.1 Tobra Formation

The Tobra Formation is made up of pebbles, boulders, and gravels, including igneous rocks in sandy, silty and muddy matrices. Gravels and Pebbles are generally pink granite and sometimes metamorphic rocks. The matrix has silty and clay properties. Shales are predominantly dark gray to gray green in color (Moghal et al., 2007).

The main deposition environment of the stratum is the glacier-ocean environment, which sometimes becomes shallow sea in some places. The igneous rock fragments appear to originate from Mount Kirana and Rajasthan, and the slate fragments appear to originate from the metamorphic belt of northern Pakistan.

Tobra Formation sandstones are primarily horizontal and vertical fissures.

2.7.2 Dandot Formation

Sandstone with infrequent thin pebbly beds and secondary splintery shales are present. It is usually deposited in marine environment (Shah, 2009).

2.7.3 Warcha Sandstone

The Formation comprises dominantly of light brown to pinkish white arkosic sandstones. They intercalate comparatively thin and dark brown shale which are fine to coarse grained and are medium to thick bedded (Hussain, 1967). The Formation is locally spotted. It has some carbonaceous shale with irregular coal seams in western salt range but the chance of Warcha sandstone to be a source rock is very poor (Shah, 2009).

2.7.4 Sardhi Formation

Sardai Formation comprises of greenish and bluish grey clays with some slight siltstone beds (Gee 1935, Eames et al, 1952). The facies deposited are prominent and vary from mainly lavender color clays in salt range to black agrillaceous limestone in the Khishor range.

2.8 PALEOCENE

The regression of sea marks the end of the Mesozoic era in most of Pakistan. This phenomenon is most prominent in the Khairpur-Jacobabad highlands in the Upper Indus basin and in the Suleyman and Kirthar basins.

In the Upper Indus Basin, the Paleocene strata are known as the Hangu Formation, Lockhart Formation, and Patala Formation. The Hangu Formation cannot be identified in that part of the Potwar Basin that was eroded after deposition and can only be identified when the outcrop shows a residual sedimentary environment.

2.8.1 Lockhart Formation

This Formation comprises mostly of limestone. The limestone varies in color from grey to light grey and in lower part has medium bedded nodular dark bluish grey calcareous shale (Gee 1933, Eames et al, 1952). Lockhart Formation in eastern Potwar to some level has established some rock for soil generation.

2.8.2 Patala Formation

Shale and marl with subordinate limestone and sandstone are present in the Salt Range. The shale is of dull greenish dark selenite-bearing, calcareous and carbonaceous in spots and moreover comprises marcasite nodules. The limestone is nodular, interbedded and is of white to light dark in colour. In the upper part there are subordinate interbedded yellowish brown and calcareous sandstone (Gee, 1989).

2.9` EOCENE

The single most significant epoch in the geological history of Pakistan is Epoch as it has presented the highest vintage of hydrocarbon especially Eocene carbonate reservoir have been most important commercially (Shah, 2009).

2.9.1 Sakesar Limestone

The section consists of limestone, thin shale and marl beds. This limestone varies in color from light to dark brown, olive brown and whitish to light grey (Gee, 1935).

This Formation has cuttings which are angular, hard, blocky locally fractured and splintery. The Formation makes confirmable upper contact and lower contact and has a shallow marine or lagoonal environment of deposition (Shah, 2009).

2.9.2 Chorgali Formation

Formation is separated into two sections in Salt Range. The lower part comprises shale and limestone, while the upper part is of limestone. The shale is of light green, calcareous, and the limestone is of dim dark and argillaceous, the Formation comprises of huge beds (Shah, 2009).

2.10 MIOCENE

This system is basically controlled in north by the Himalayan orogeny related tectonic activities and in the west by the origin of axial belt, as a result of collision between Eurasian and Indian plates (Shah, 2009).

Upper Indus basin whole area was uplifted. These fresh water molasse deposits are signified by the Formations which are as follow

2.10.1 Murree Formation

The Formation is composed of succession dark red and light purple and light greenish sandstone with subordinate intra Formational conglomerates. There are light greenish dim calcareous sandstone and conglomerates with plentiful inferred bigger foraminifers of Eocene age in basal strata of the Formation (Shah, 2009).

2.10.2 Kamlial Formation

Kamlial Formation is comprised of red and light purple sandstone which is of medium to coarse grained and comprises interbedded hard purple shale, yellow and purple intra-Formational conglomerate. It is recognized from Murree Formation by its normal spheroidal weathering and minerals content where tourmaline replace epidote (Shah, 2009)

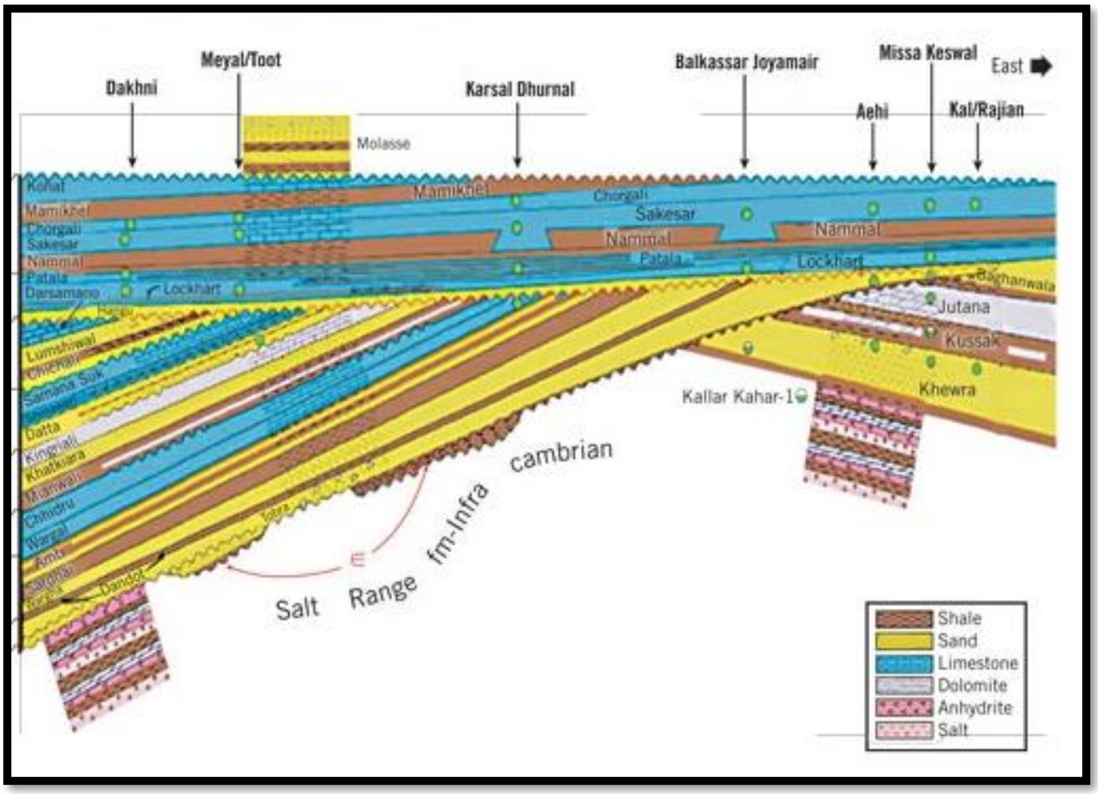

Figure 2.2 Generalized schematic stratigraphic map of the Upper Indus Basin. (Moghal et al, 2007)

2.11 REGIONAL TECTONICS

Potwar Sub-basin is regarded as one the most established and old oil and gas zones which is famous for its triangle plays. It is in western Himalayas, in northern Pakistan. Potwar Plateau, Salt Range, Jhelum plain are a part of this area. Due to the subduction of Indian plate sedimentary record in the subsurface has been decoupled. Large number of thrusts, back thrusts and nappes are observed in the study area due to the tectonic arrangement (Butler et al., 1988).

A distorted sedimentary sequence aging from Pliocene to Pleistocene is found in Kohat-Potwar foreland basin. Main boundary thrust form its northern boundary, Salt range thrust forms its southern boundary, and Kalabagh Fault is present in west and

Jhelum Fault is present in the east. Portion between Jhelum Fault and Kalabagh Fault is called Potwar Sub basin and west of Kalabagh fault between SRT and MBT is called Kohat Sub basin. In the west of Kalabagh Fault and Surghar ranges are present and below it Khisor ranges are present. Ranges between two rivers (Jhelum and Indus) is called Cis-Indus Ranges and Surghar and Khisor Ranges are called Trans-Indus Ranges (Khan et al., 1986)

2.12 POTWAR SUB-BASIN

Pakistan is mainly composed of two major basins geographically, Indus and Baluchistan basin. Indus basin is further subdivided into Upper Indus basin, Lower Indus basin and Central Indus basin. Lower Indus basin is separated from Upper Indus basin by Sargodha highs. Upper Indus basin is further subdivided in to two basins, Potwar Sub Basin and in the west as Kohat Sub Basin. Precambrian to Quaternary age sediments are preserved in Potwar sub-Basin. As shown in figure 3.1 Fimkassar is located in the eastern Potwar region, and this area has a very complicated tectonic framework. Eastern Potwar is divided into two segments, SPDZ (Southern Potwar deformed zone, area between SRT and Soan Syncline) and NPDZ (Northern Potwar deformed zone: area between Soan Syncline and MBT) (Butler et al., 1987).

NPDZ is a foreland fold and thrust belt found in the northern Potwar region. Salt is the major lithology controlling all tectonic activity in the thicker SPDZ. Ductile behavior is shown by salt and the tectonic activity associated with salt in this region is known as thin skin tectonic. It is a type of tectonic activity in which salt or gypsum act as a ductile material and results in brittle Deformation of overlying hard rocks. Basement is not involved in the tectonic activity hence SRT is known as decollement or detachment fault, allowing no Deformation below the basement (Butler et al., 1987).

2.13 GEOLOGICAL FRAMEWORK

Fimkassar area lies in Eastern Potwar. The region shows very active tectonic framework with observable low angle thrusts and back thrusts showing immense shortening found in any other region. Eastern Potwar has most of the folds with direction of NE-SW and very few EW trending folds in the focal district. Imbricate thrusts, popup structures and triangle zone are found over here. Fault limited hydrocarbon traps are found in the region due to over thrusting and shortening like Domeli back thrust, Dill Jabba fore thrust and SRT (Khan et al., 1986).

Apart from the Salt Range Thrust found in the south, a second important thrust is Domeli thrust fault in the eastern Potwar. This Domeli thrust is predicted to be a foreland-verging thrust which demonstrates a great deal of shortening. The Potwar basin is bounded by Domeli thrust in the east (Pennock et al., 1989).

Domeli back thrust is the most common back thrust found in eastern Potwar. The structure present in Fimkassar area is a fault limited anticline. Other fundamental structural faults are compensating their separation level which occurs in Precambrian salt (Aamir and Siddiqui, 2006).

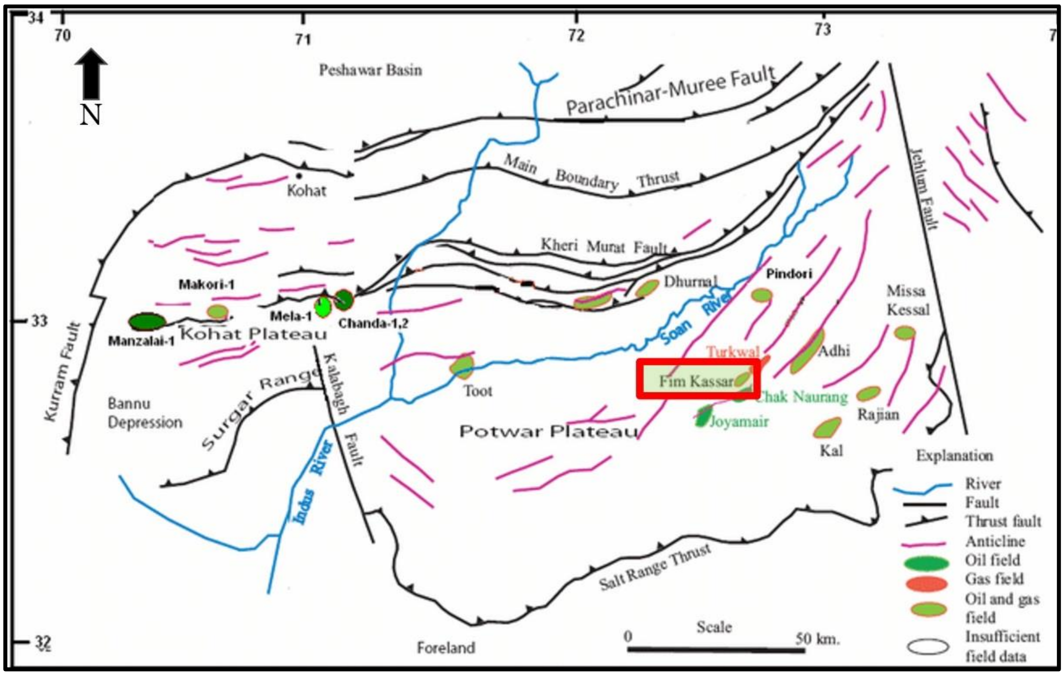

Figure 2.3. Structural map of Kohat-Potwar Plateaus, Northern Pakistan (Gee and Gee, 1989).

2.14 TECTONIC BOUNDARIES OF POTWAR PLATEAU

The Potwar sub basin is structurally arranged on south of western lower regions of Himalayas. Main Boundary Thrust (MBT) bound it in the north, Salt Range Thrust (SRT) in the south, Jhelum fault in the east and Kalabagh fault in the west (Najman et al., 2003). As shown in figure 2.1 the Potwar is bounded by two strike-slips in the east and two thrust faults which are as under (Shah, 2009).

2.14.1 Kalabagh fault

It is situated in the north of the Kalabagh city, Mianwali and right lateral strike slip (dextral) fault. Its direction is north to west 150 km. Separates Cis and Trans-Indus Ranges of Western Salt Range (McDougall and Khan, 1990).

2.14.2 Jhelum fault

Left lateral (sinistral) Jhelum Fault in west extends from Kohala to Azad Pattan. Murree Formation is on hanging wall while Kamlial, Chingi and Nagri Formations are present on the foot wall. After crossing Chattar area in Muzaffarabad, Jhelum fault run parallel to the Jhelum River in north south direction and exhibits a sharp contact in most of its exposures (Baig, 2006).

2.14.3 Salt Range Thrust (SRT)

Salt Range Thrust is a complex salt anticlinorium known as Himalayan Frontal Thrust. Trans-Indus Himalayan and Salt Range are the foothills (DiPietro and Pogue, 2004).

2.14.4 Main Boundary Thrust (MBT)

MBT which lies to the north of the Islamabad is called as Murree Fault. Main Boundary Thrust is the continuation of Hazara Kashmir syntaxes and forms the Southern boundary of Himalayan Deformation form MMT (Coward, 1983).

2.15 HYDROCARBON POTENTIAL

Salt Range Potwar Foreland Basin (SRPFB) is an enveloped super-continental basin, accounting for 48% of the known oil and gas in the world. There are several features that lead to accumulation of hydrocarbon, comprising continental margins, thick marine sedimentary sequences, potential sources, reservoirs, and seal rock (Iqbal, 1995).

2.16 PETROLEUM SYSTEM OF AREA

Region of Kohat-Potwar fold belt is very productive for hydrocarbons as it have many petroleum systems which are proven.

Table 1. Petroleum system of the area.

Source rocks	Patala and Khewra Formation Shales
Reservoir rocks	Sakesar Limestone and Chorgali Formation
Cap rocks	Murree Formation
Trap	Structural traps

2.16.1 SOURCE ROCKS

In the Potwar sub-basin, the chief bedrock is the Paleocene Patala shale, partially deposited under anoxic situations due to folding of the bottom of the basin. The oil shale interval also exists in the Precambrian Salt Range and represents source rock potential (Shah, 2009).

The Khewra Formation is composed of shale from the lake to marine facies, proficient of producing paraffin from normal crude oil and natural gas (Petro Consultants, 1996). The Patala Formation is the key bedrock in the study area.

2.16.2 RESERVOIR ROCKS

The hydrocarbon producing strata on the Potwar Plateau include Cambrian jutana. Kherwa and Kussak; Permian Wargal, Tobra and Amb; Jurassic Data; Cretaceous Lumshiwal; Paleocene Lockhart. Patala, Nammal; Eocene Bhadrar, Chorgali, Sakesar and Margala Hill Limestone and Miocene Murree (Khan et al., 1986; Petro consultants, 1996). The main reservoir area Chorgali and Sakesar Limestone in the study area.

2.16.3 CAP ROCKS

The seal includes the fault cut and interbedded shale. For Lower Cambrian reservoirs, thick evaporation layers and shale layers offer good sealing potential. For the Cenozoic and Mesozoic reservoirs, the potential seals are limestone and shales. The regional cap rocks in this area are the Paleocene shales (Patala Formation) and the Miocene shales. Miocene Murree group provided cap rocks in study area (Shah, 2009).

2.16.4 TRAP

In the postwar sub-basin, stratigraphic and structural traps are possible. East Potwar exhibits, salt pushes and anticlines, and local pop-ups. The characteristic trend of the anticlines in the study area is usually west-southwest to east-northeast, roughly parallel to the plate collision zone (Shah, 2009).

CHAPTER 3

SEISMIC INTERPRETATION

3.1 INTRODUCTION

Seismic data interpretation refers to the qualitative and quantitative analysis of seismic section. Seismic Interpretation is a tool which help us bringing the geological and subsurface Information in form of images and models which will let us see the anomalies inside the Earth.

Seismic is an indirect method as it involves generation of models that are based on the reflections coming from the sub-surface. The objective of this modeling is to capture a structure feasible to accumulate hydrocarbon e.g., an anticline. Seismic analysis of structure is the search for structural traps that accumulate the hydrocarbons. The time contour map shows the underlying geometry of modeled horizons that have been converted to depth contour map using acceptable velocity. The focus is on finding the most suitable position for hydrocarbon collection in oil and gas exploration.

3.2 SEISMIC INTERPRETATION APPROACHES

There are two main approaches to analyze the seismic data.

1. Stratigraphic Analysis
2. Structural Analysis

5.2.1 Stratigraphic Analysis

Seismic section division into reflections sequence involves stratigraphic analysis that is interpreted as a seismic expression of genetically connected sedimentary sequences. These characterize variation in the sedimentary deposition.

3.2.2 Structural analysis

Structural traps are mainly focused in structural analysis in which important part is played by tectonics. The main purpose of structural analysis is to look for possible structures that can embrace and accumulate hydrocarbons. The interpretation techniques that are used in many structural interpretations is two-way reflection times than depth. Fold, faults, and anticlines are main concern in this approach. (Kearey, 1988)

Structural analysis approach was followed for interpretation.

3.3 WORKFLOW FOR SEISMIC INTERPRETATION

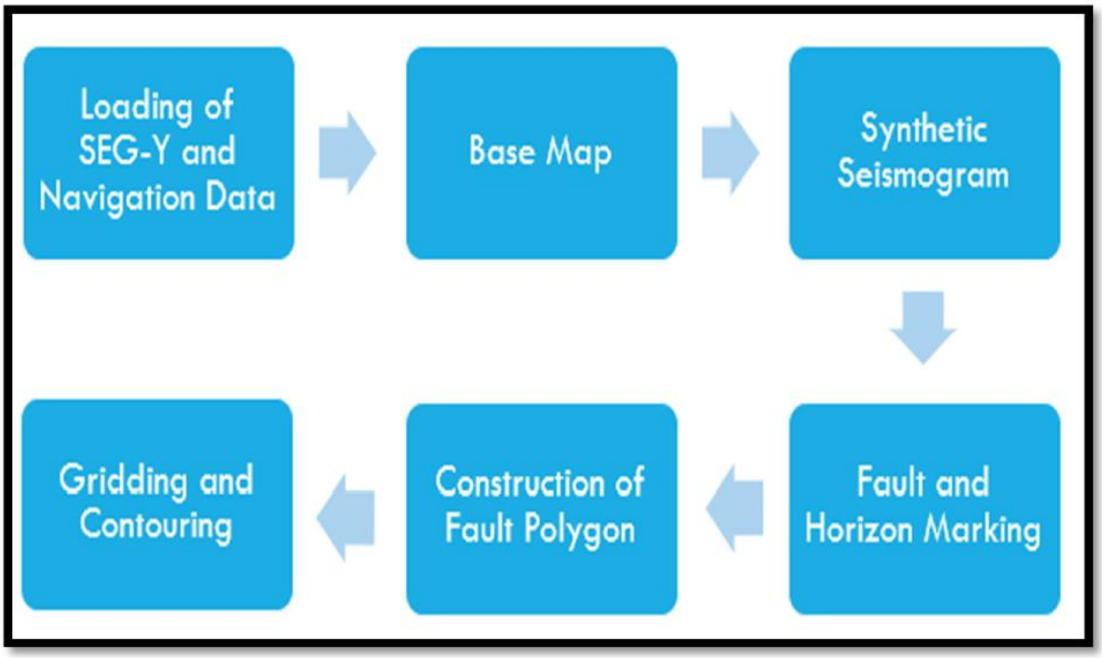

Figure 3.1 workflow of seismic interpretation

3.3.1 Loading of data

The first step in seismic interpretation is loading of the digital data. Having two types of data well data and reflection data, first will load both into our new project. The interpretation work was carried out on Kingdom Suit and the first process was loading of the navigation files provided by DGPC and assign the correct UMT zone for data. After loading of navigation files all the six seismic lines SEGY were loaded into the program using batch mode. After successfully loading of reflection data both Wells were loaded using their well coordinates, well tops, time-depth chart, and Las files.

3.3.2 Base Map

Base map is a graphical description of all the data set which will be used during the research work. Figure 3.2 shows the base map of study area which shows six seismic lines and two wells.

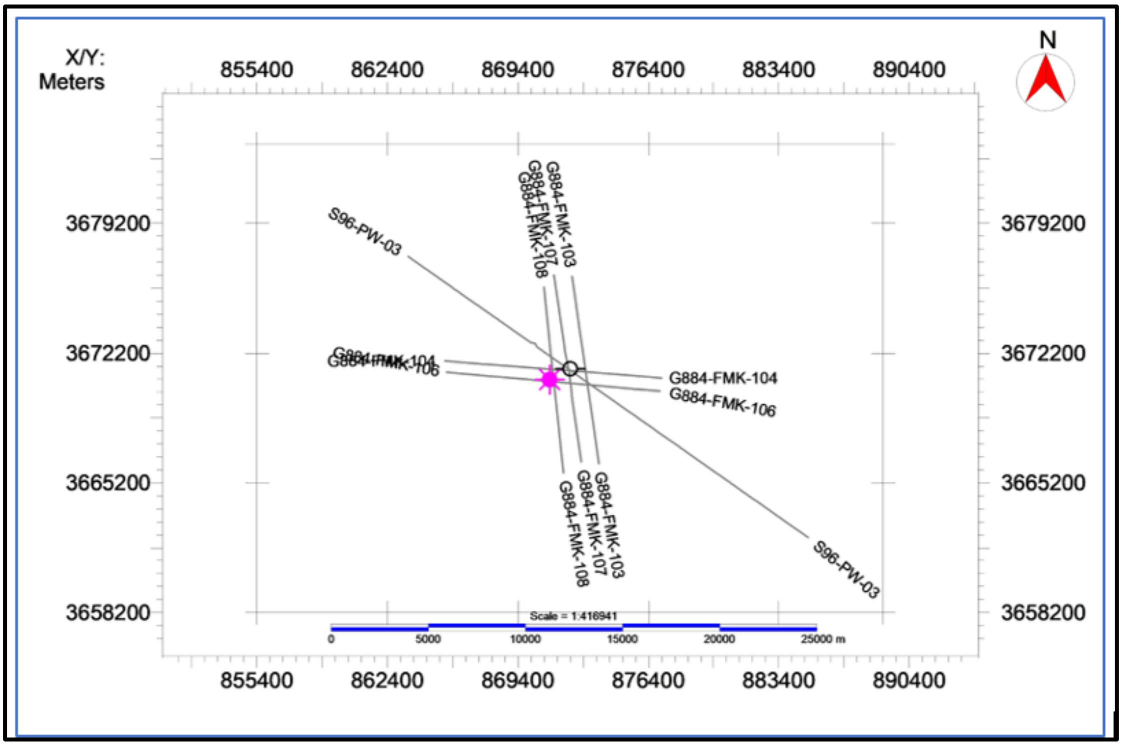

Figure 3.2 Base map of study area

3.3.3 Generation of Synthetic seismogram

Synthetic seismograms provide a crucial link between lithological variations within a drill hole and reflectors on seismic profiles crossing the site. In essence, they provide a ground truth for the interpretation of seismic data. Synthetic seismograms are useful tools for linking drill hole geology to seismic sections because they can provide a direct link between observed lithology's and seismic reflection patterns (Handwerger et al., 2004).

After both the wells were successfully loaded at its true position, the next step is construction of synthetic seismogram. The synthetic seismogram helps in comparing well data with seismic data for identification of reflectors near the wellbore. It is created by using the sonic log (DT) and density log (RHOB). the product of sonic log and density log gives acoustic impedance i.e.

Acoustic impedance Z = ρ* V

After Z is calculated, reflection coefficient (RC) series is generated. The RC series represents nature of reflections when reflected back from a boundary. It is calculated by

$$\mathbf{RC = (\rho_2 V_2 - \rho_1 V_1) / (\rho_1 V_1 + \rho_1 V_1).}$$

Where RC = reflection coefficient, whose values range from −1 to +1

ρ_1 = density of medium 1 display wavelet

ρ_2 = density of medium 2

V_1 = velocity of medium 1

V_2 = velocity of medium 2 These are independent of a waveform.

Extracted source wavelet is then convolved with RC series to produce a Synthetic seismogram.

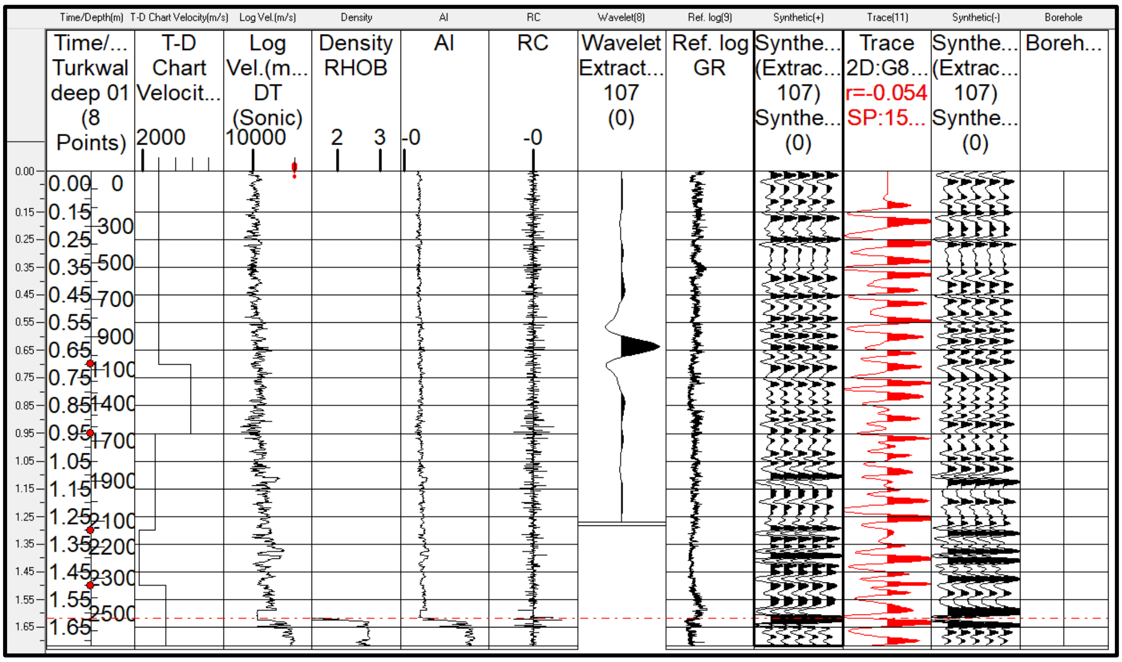

Figure 3.3 Synthetic seismogram of Turkwal Deep 01

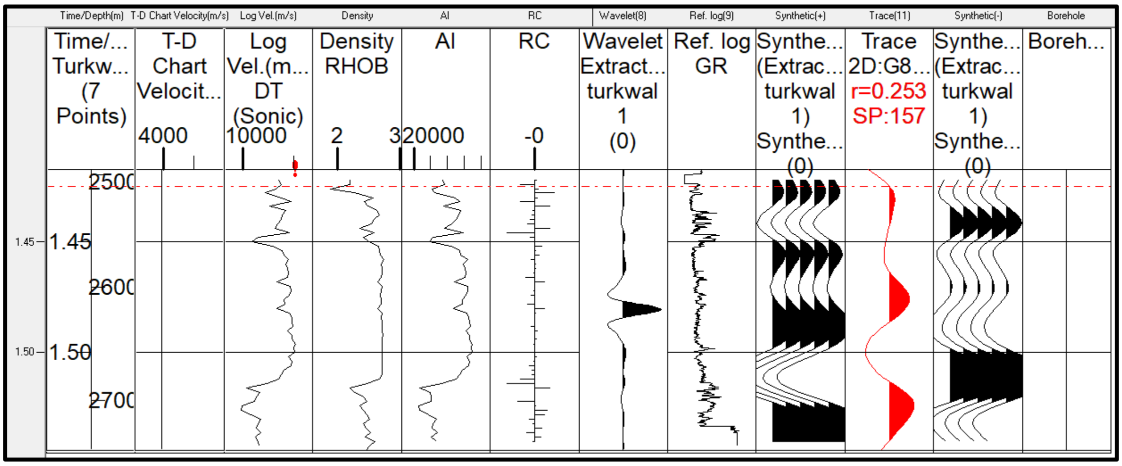

Figure 3.4 Synthetic seismogram of Turkwal 01

3.3.4 Well to seismic tie

The correction of the datum was performed to set seismic and well data to the same reference datum. Formation tops are estimated from kelly bushing (KB) and seismic data is acquired in seconds from seismic reference datum (SRD). The following corrections are applied to bring Formation tops from well to seismic datum.

TVD seismic (True vertical depth) = Formation top – KB + SRD

In the study area, SRD=MSL, where mean sea level (MSL)=0 meter. So, Formation top was only subtracted from Kelly bushing (KB)

3.3.5 Horizon Interpretation

Seismic Horizons are vertical discontinuities of geological Formations. The main part of seismic interpretation is to recognize seismic horizons which are marked based on acoustic impedance contrast. The 2D seismic interpretation is done using SWT kingdom software. Before moving to seismic interpretation a interpreter should have enough knowledge of the geology of the area and which Formations act as reservoirs.

After in depth study of the area it is resulted that sandstones and limestones of Eocene till Cambrian act as reservoir zone in Upper Indus Basin; selected Chorgali Formation of Eocene and Khewra Sandstone Formation to be marked as our primary reservoir in study area.

After selection of the horizon to be marked the next step is identifying them of seismic data and for that help was taken of the well data. Than will use the TD chart which was made with help of interval velocity and depth from well data and validate our time of horizons from synthetic seismogram.

Table 3.1 TD chart of well Turkwal-01

Depth (m)	**Time (sec)**	**Formation**
0	0	Nagri
710	0.12246	Chinji
1662	0.68451	Kamlial
1865	0.79065	Murree
3021	1.42492	Chorgali
3067	1.44829	Sakesar
3192	1.51178	Patala
3218	1.52498	Lockhart
3230	1.53108	Hangu
3239	1.53565	Sardhai
3245	1.5387	Warcha

Table 3.2 TD chart of well Turkwal Deep-01

Depth (m)	**Time (sec)**	**Formation**
0	0	Nagri
563.9	0.02806	Chinji
1529.4	0.67173	Kamlial
1731.2	0.76506	Murree
3049.1	1.61899	Chorgali
3103.5	1.65099	Sakesar
3198.7	1.70699	Nammal
3225.8	1.72294	Patala
3250.8	1.73764	Lockhart
3261.8	1.74411	Dhak Pass
3265.2	1.74611	Sardhai
3382.8	1.8165	Warcha
3427.6	1.84495	Dandot
3462.4	1.86704	Tobra
3505	1.89409	jutana
3523.3	1.90571	Kussak
3539.2	1.9158	Khewra Sandstone
3605.63	1.95798	Sakesar 2
3633	1.97536	Salt Range
3822	2.09536	Murree

4311.2	2.37655	Chorgali 2
4360.9	2.39151	Sakesar 2

The selected Formations to marked are as follows

Table 3.3 Selected Formations to mark

Formation	**Time (sec)**
Chorgali	1.61
Khewra Sandstone	1.91
Chorgali 2	2.37

3.3.5.1 Selection of control Line

In order to mark horizon and faults properly on all seismic lines. There must be a control line with which other lines are tied and well must be present on that line. As the Turkwal deep 01 lies on line 884-FMK-107 and Turkwal-01 on 884-FMK-106 so these both lines were taken as control lines.

3.3.6 Fault Interpretation

Conventional seismic interpretations are the arts that require skills and thorough experience in Geology and Geophysics to be precise (Mc. Quillin et al., 1984). Fault marking on real time domain seismic section is quite a hard work to do without knowing tectonic history of Area (Sroor, 2010). Faults are marked based on breaks in the continuity of reflection. This Discontinuity of the reflector shows that the data is disturbed here due to the passing of the faults.

Fimkassar lies in the upper Indus Basin so that is compressional regime so reverse thrust faults will be visible in area followed by anticlines and synclines. There can be normal faulting in basement due to compression.

3.3.7 Contour maps

On a 2D map line showing the same parameter such as depth, elevation is known as Contour map. The contours here are generated with the help of values of time, which is the time taken by the wave to reflect back because of contrast of acoustic impedance from noticeable dense reflector. On a map, contours of time are generated for each reflector by taking the values of reflector time picking on the line. In my study Chorgali Formation and Khewra sandstone are reflectors of interest which are plotted on the contour sections mentioning to these reflectors' reflection time values.

TWT contours are representing the line which have same values of time. It is the time which is consumed by the seismic wave to move from source to the subsurface then strike a surface and reflect to the surface. Latitude/longitude values of every shot point are given on Base map. For each horizon, time grid is generated which is represent marked horizon time in different colors.

3.4 INTERPRETTED SEISMIC SECTIONS

The interpretation started on the control line 884-FMK-107 which is our main dip line of the area and the other control line which is 884-FMK-106 which is the strike line

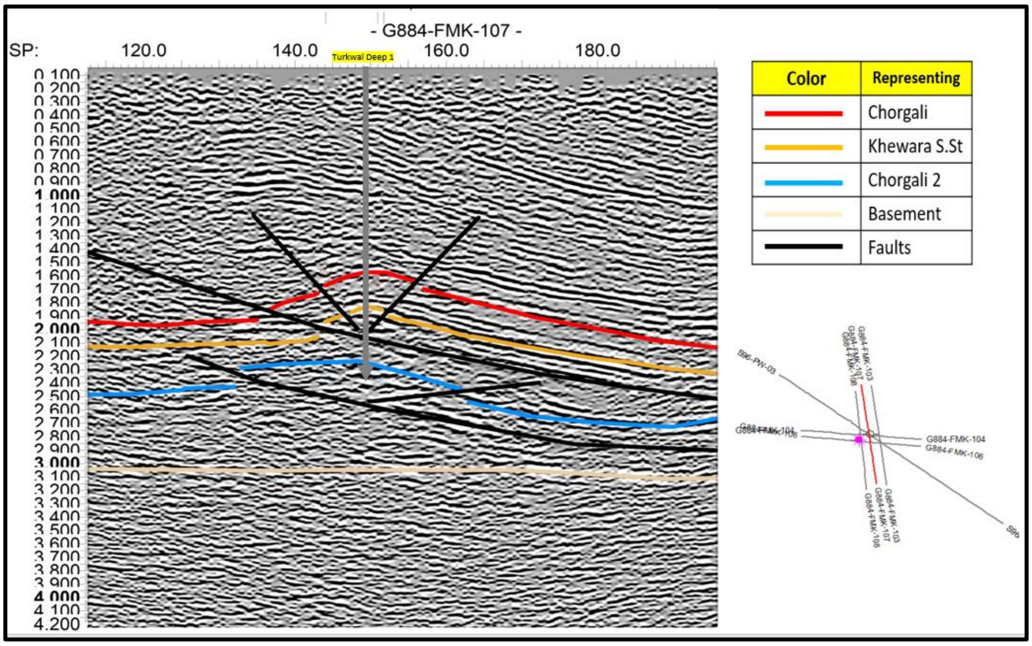

Figure 3.5 Interpreted Seismic section of 884-FMK-107

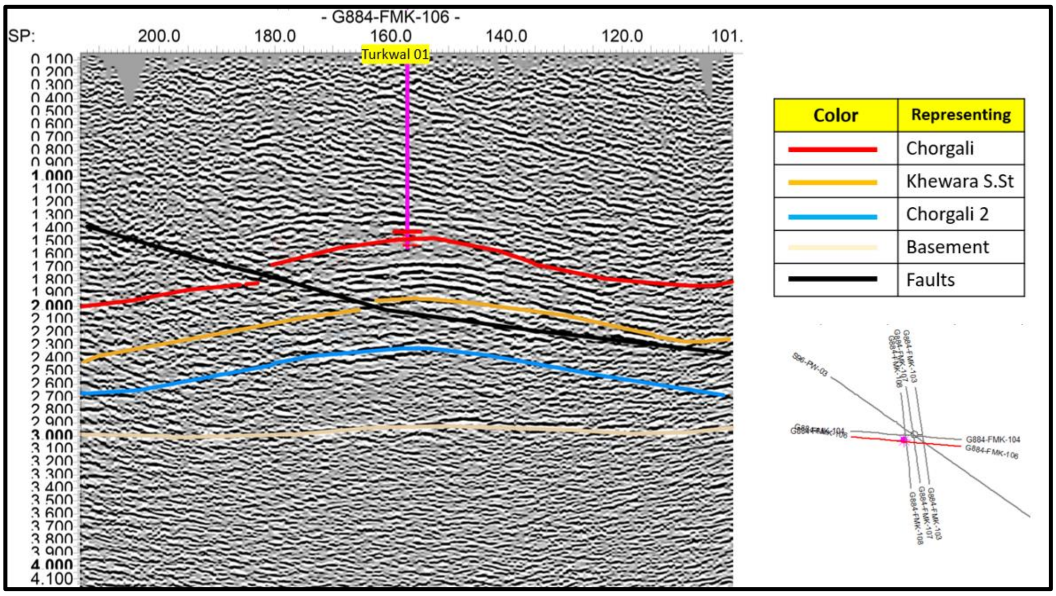

Figure 3.6 Interpreted Seismic section of 884-FMK-106

Above both the lines are control lines from these two lines we have generated our geological model and using this geological model we will corelate the interpretation on remaining lines using tie points and jump correlation. But before doing interpretation on other lines an important task is to remove the Mistie from each section by looking towards the control line. So, after removing the Mistie next step is to take control from tie points and continue the interpretation keeping in mind the geological model. The interpreted seismic sections are as follows

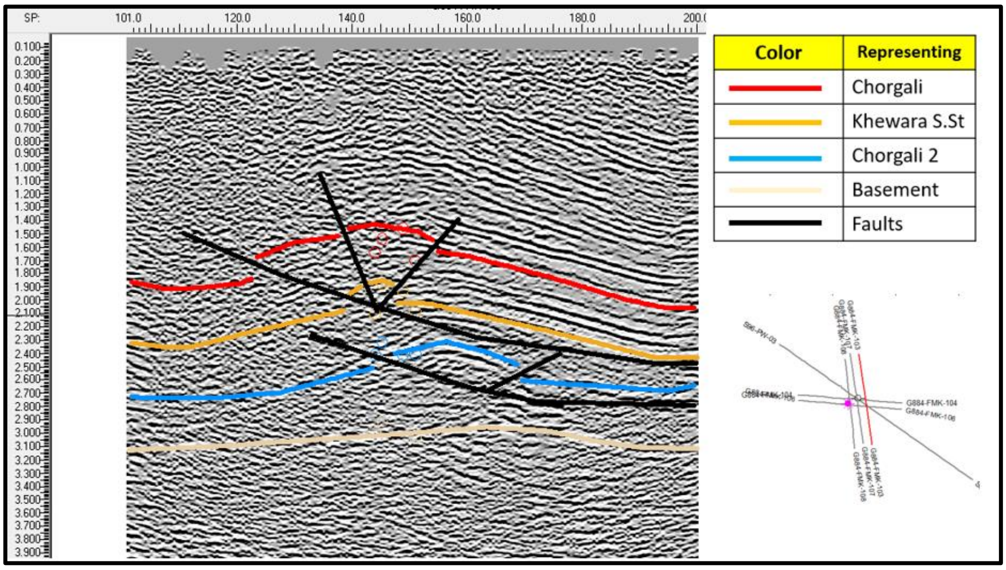

Figure 3.6 Interpreted Seismic section of 884-FMK-103

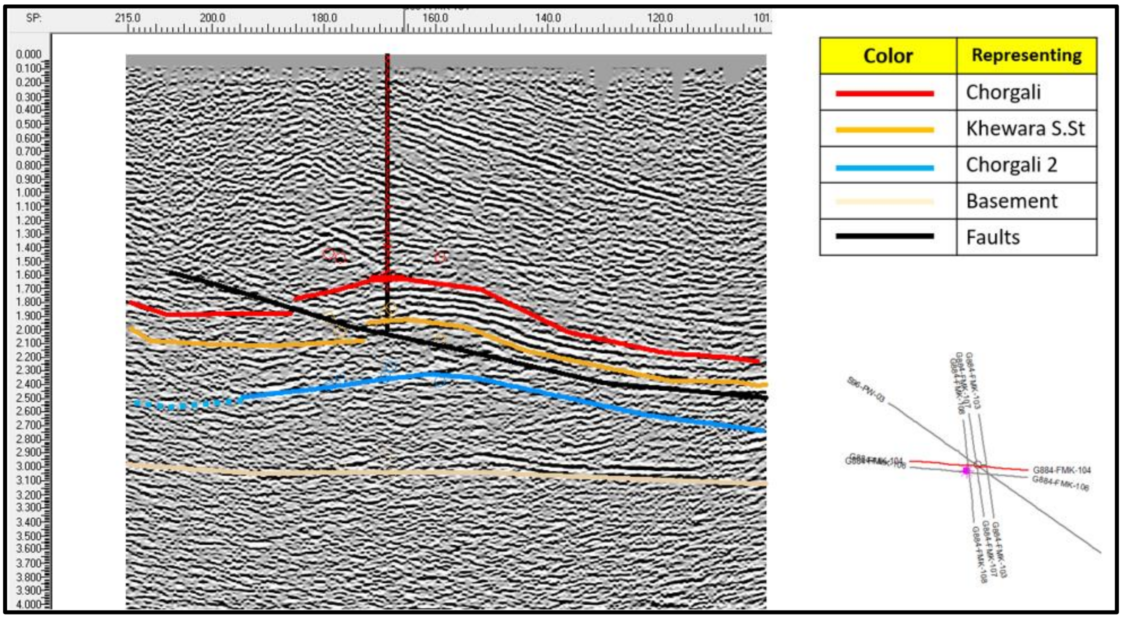

Figure 3.6 Interpreted Seismic section of 884-FMK-104

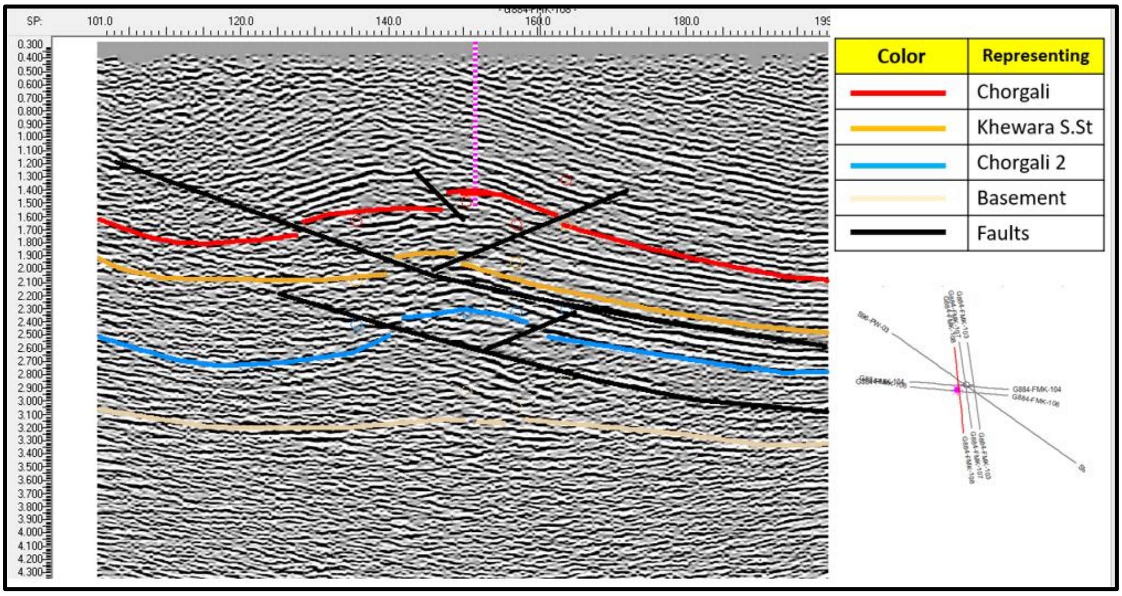

Figure 3.6 Interpreted Seismic section of 884-FMK-108

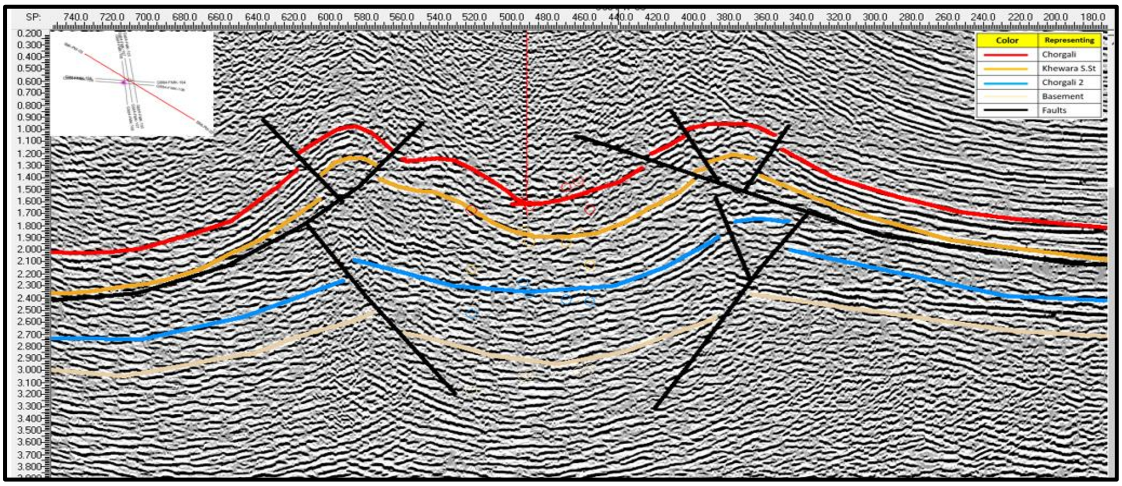

Figure 3.6 Interpreted Seismic section of 96-PW-03

3.5 TIME CONTOUR MAP

Contour map is generally defined as the line showing the same parameter (depth, elevation) on a 2D map. Here, the contours are made with the help of the time values, which is the time of the wave to reflect from a prominent dense reflector or strata due to the acoustic impedance contrast. For each reflector on the map contours of time are generated, taking values of reflector time picking on the line. In case of our study, the reflectors of our concern are Chorgali Formation, Khewra Sandstone and second sheet of Chorgali Formation and these are plotted on the contour section referring to the reflection time values of these reflectors.

3.5.1 Fault polygons

Faults interpretation plays an important role in seismic interpretation but more important is fault correlation. Once faults are marked on all seismic sections than corelate same faults on base map and join them to form a polygon so in that way we know the orientation of the subsurface structure.

Below three, time contour maps figs 3.7, 3.8 and 3.9 are representing time contour maps of Chorgali Formation, Khewra Sandstone and second sheet of Chorgali Formation

The trend of contour in maps is validating the interpretation done on seismic lines it is showing an anticlinal faut bounded structure on which the well is marked.

The Jhelum left lateral strike-slip fault in the east and the right lateral strike-slip Kalabagh fault in the west have played pivotal role in shaping the geometry of the Fimkassar Area. Due to these faults, the structures in the eastern part of the study area are left stepping whereas in the western part right stepping En-echelon aligned.

The maps have made it clear that how Salt Range Thrust has brought the entire sequence over the Quaternary and is deepened towards the north side in our study area. The presence of normal faults in the basement have also helped in structural Formation in sub-basin. The overall trends in the map are confirming Pop-up anticlines, triangle zones, snake-head anticlines and salt cored anticlines.

3.5.2 TWT contour map of Chorgali Formation

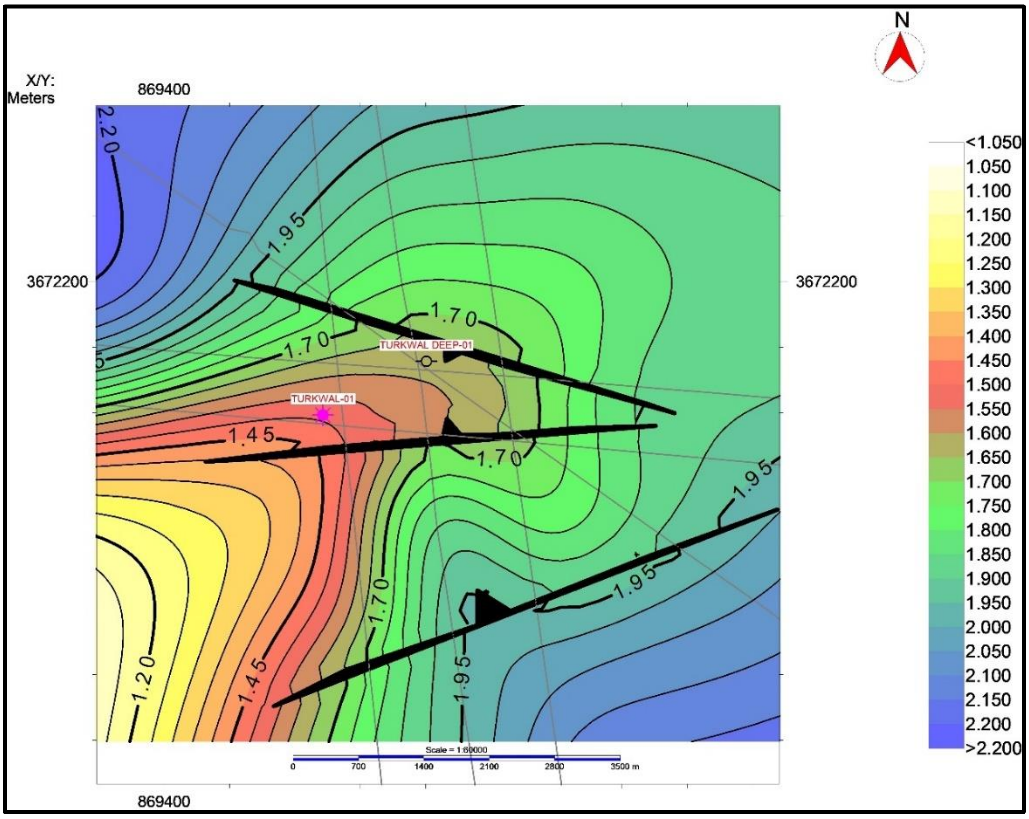

Figure 3.7 Contour map of Chorgali Formation

The figure above is showing anticline structure. The seismic lines have also confirmed the presence of three major faults which are represented by black lines. As these maps are of first sheet of Chorgali encountered so it is showing time ranges between 1.5-1.7sec in which Eocene was found.

3.5.3 TWT contour map of Khewra Sandstone

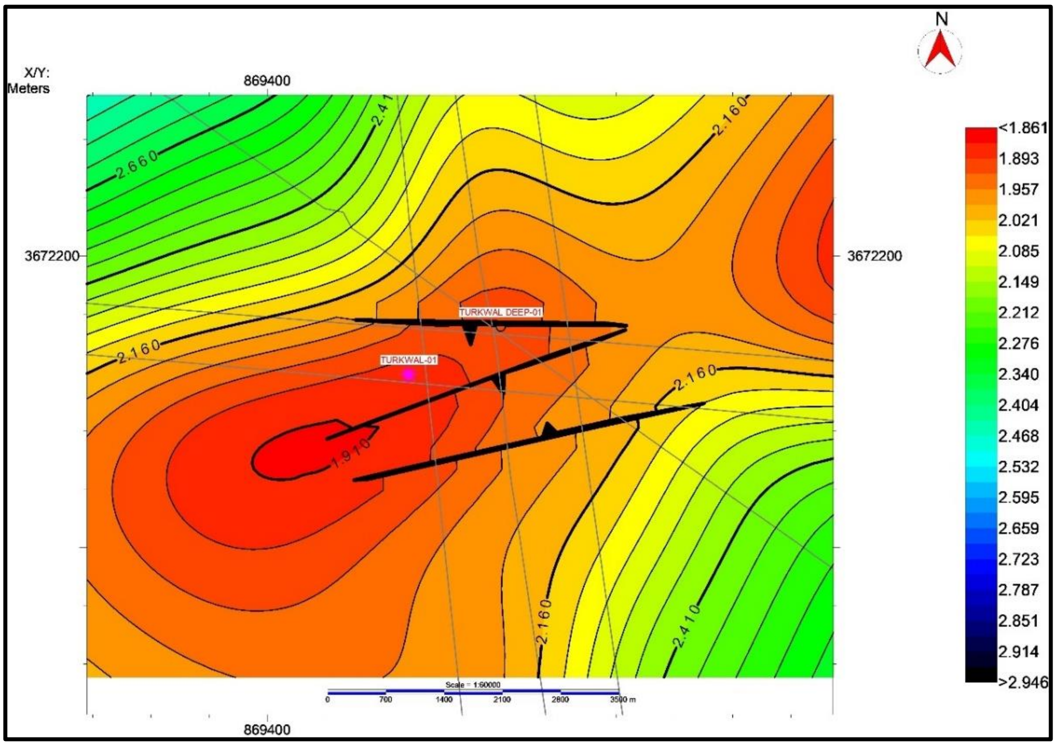

Figure 3.8 Contour map of Khewra Sandstone

The figure above is showing anticline structure for Khewra Sandstone same as for Chorgali Formation. The seismic lines have also confirmed the presence of three major faults which are represented by black lines. As these maps are of Khewra Sandstone so it is showing time ranges between 1.9-2.0 sec in which Eocene was found.

3.5.4 TWT contour map of Chorgali 2 Formation

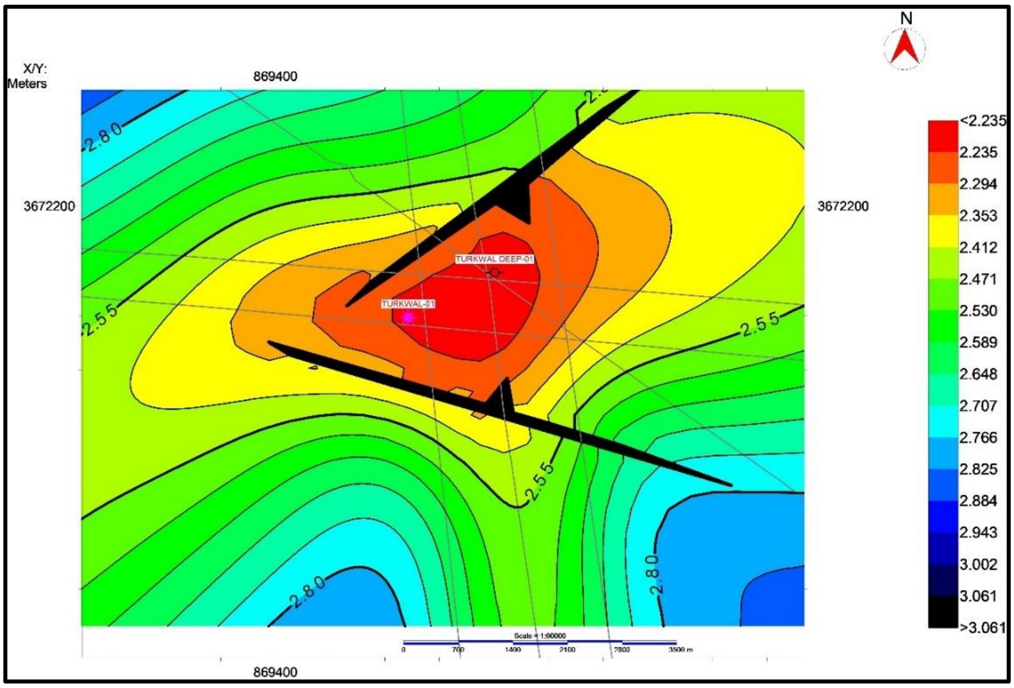

Figure 3.7 Contour map of Chorgali 2 Formation

The figure above is showing time contour maps of second sheet of Chorgali Formation. The second and third sheets of Eocene are recorded in upper Indus Basin due to compressional tectonics. The sheets are separated by major decollement faults. The above map is showing a perfect pop-up anticline bounded by two major faults as also interpreted in seismic lines ranges between time 2.3 to 2.5sec.

3.6 DEPTH CONTOUR MAPS

Depth contour maps plays a very vital role in validating the interpretation done on seismic data. Depth maps help the interpreter compare its structure depth with depths of Formations in well tops and give exact idea for well location and depth to be drilled.

3.6.1 Velocity computation

To generate depth map, we need velocity to multiply with time to get depth. For velocity data as we will discuss in next chapter velocity modelling was carried out on every line and interpolated velocity data was exported from that model. Then using this interpolated velocity model for each line, it was than multiplied with already generated time maps in Kingdom software to get depth maps.

3.6.2 Depth contour map of Chorgali Formation

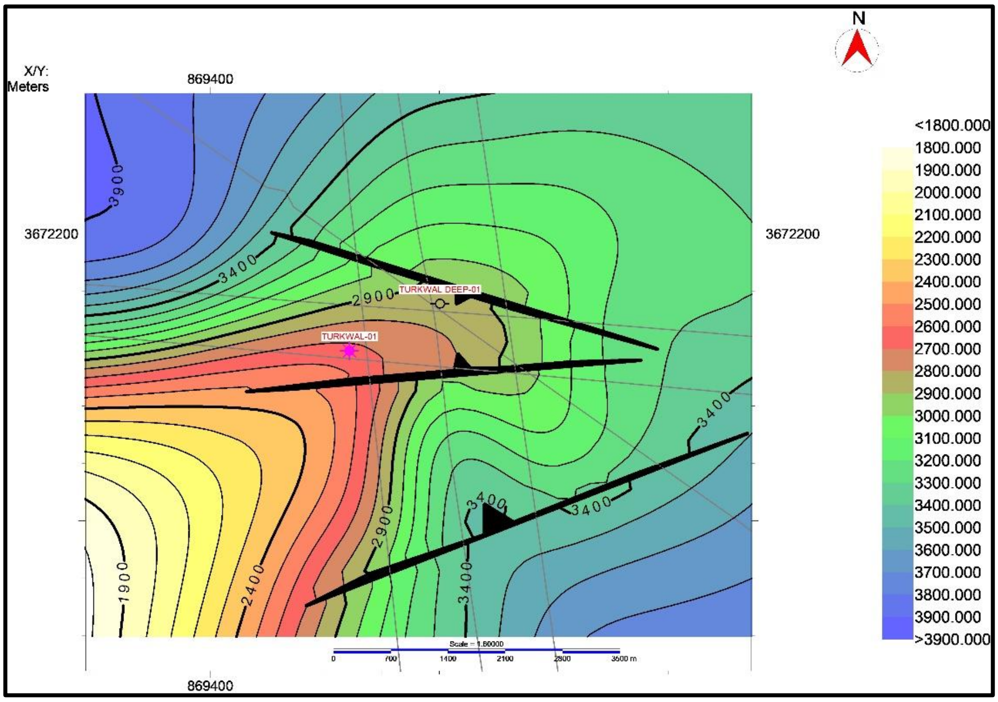

Figure 3.8 Contour map of Chorgali Formation

The figure above is showing depth contour map of Chorgali Formation. The Formation was recorded at depth of 2878 meters in well and depth maps are also validating the same depth.

3.6.3 Depth contour map of Khewra Sandstone

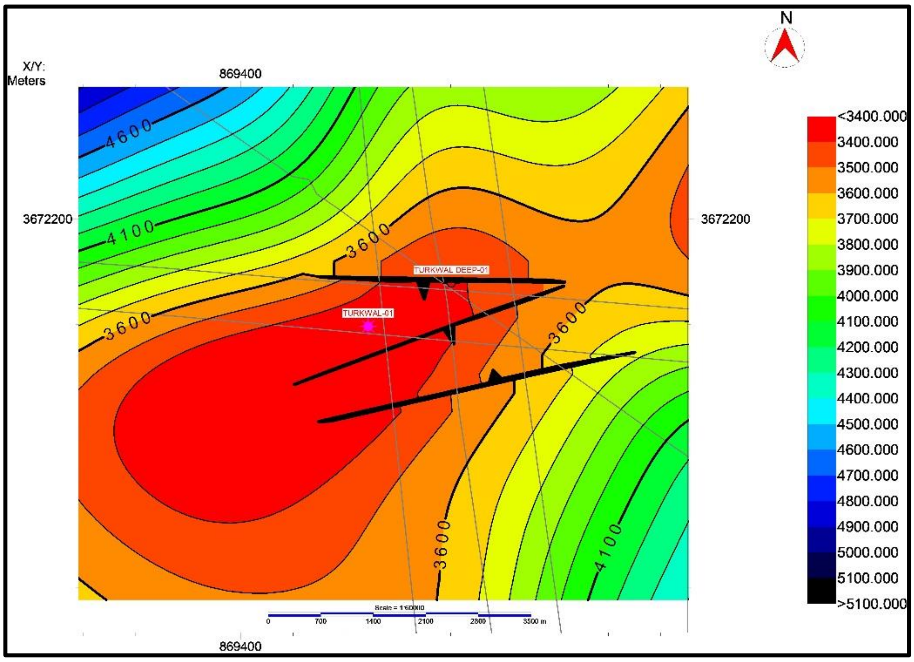

Figure 3.9 Contour map of Khewra Sandstone

The figure above is showing depth contour map of Khewra Sandstone. The Formation was recorded at depth of 3374 meters in well and depth maps are also validating the same depth.

3.6.3 Depth contour map of Chorgali 2 Formation

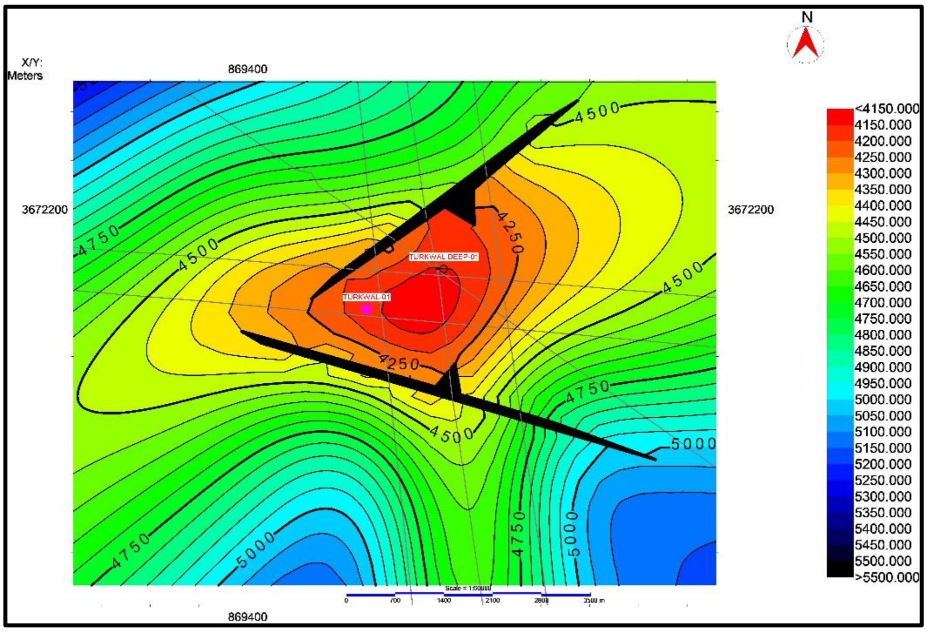

Figure 3.10 Contour map of Chorgali 2 Formation

The figure above is showing depth contour map of second sheet of Chorgali Formation. The Formation was recorded at depth of 4146 meters in well and depth maps are also validating the same depth.

The trend of contour in maps is validating the interpretation done on seismic lines it is showing an anticlinal faut bounded structure on which the well is marked.

CHAPTER 4

VELOCITY MODELLING

4.1 INTRODUCTION

Velocity model building is the most important and critical element in seismic data imaging. The demands of exploring more complex new frontiers will not be fulfilled without accurate velocity models. Understanding the fundamentals, and then challenging the approximations of seismic velocity estimations, limitations, and pitfalls in practical applications, are the main keys of building the most accurate integrated velocity model. Accurate velocities are the main challenge for improving seismic data and depth prediction. For example, near-surface irregularities require accurate velocity models for proper imaging of the deep subsurface.

A seismic velocity model is necessary to map depth and thickness of subsurface layers interpreted from seismic reflection images. Velocity modeling enables the use of velocity information from both seismic and wells, providing a much broader data set for critical review and quality control.

4.2 WORKFLOW FOR VELOCITY MODELLING

Velocity modelling is carried out in multiple steps, the flow chart showing steps involved in velocity modelling are as follows.

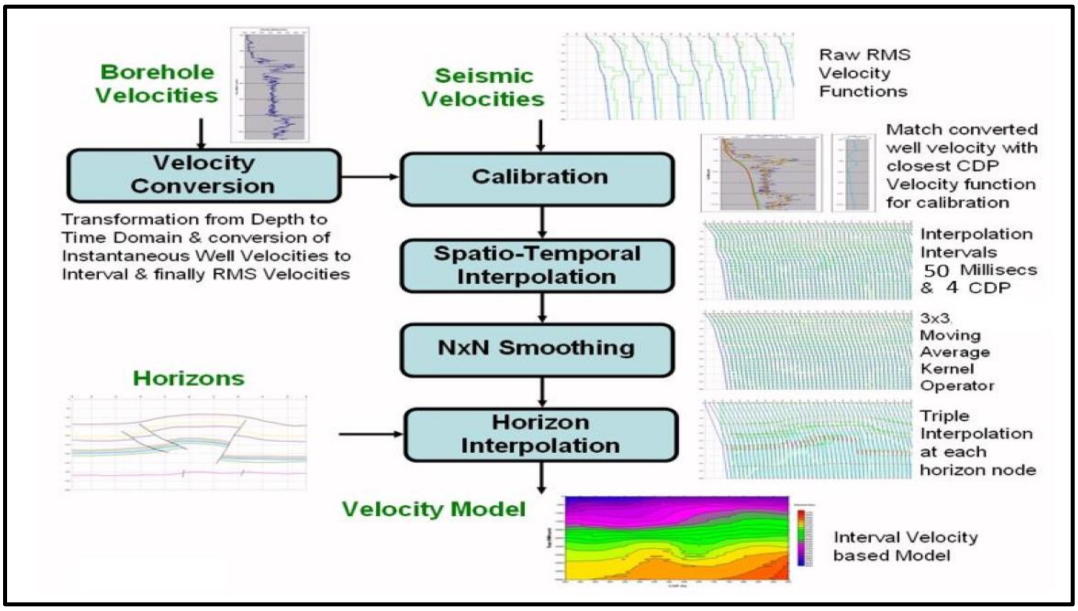

Figure 4.1 Workflow for velocity modelling

4.2.1 Velocity conversion

For velocity modelling use both velocities from seismic and well to generate a model. As well velocities are in depth domain and seismic is in time domain so our first step will be Transformation from depth to time domain and conversion of instantaneous Well velocities to Interval and finally RMS velocities.

In our case we have taken the sonic log as a function of depth from well and apply moving average function of depth than by taking the velocities from sonic we have converted it into time domain.

4.2.2 Velocity Calibration

Seismic is an indirect source of velocity information, thus seismic velocities need to be refined through calibration using more precisely measured borehole velocities. This calibration requires both seismic and borehole velocities to be in the same form in terms of resolution or sampling interval, type of velocity, and time-depth domain. Discrepancy also exists between borehole velocities from sonic logs that must be resolved before calibration (Khan and Akhtar, 2011).

The workflow of velocity calibration is shown in fig 4.2 as under

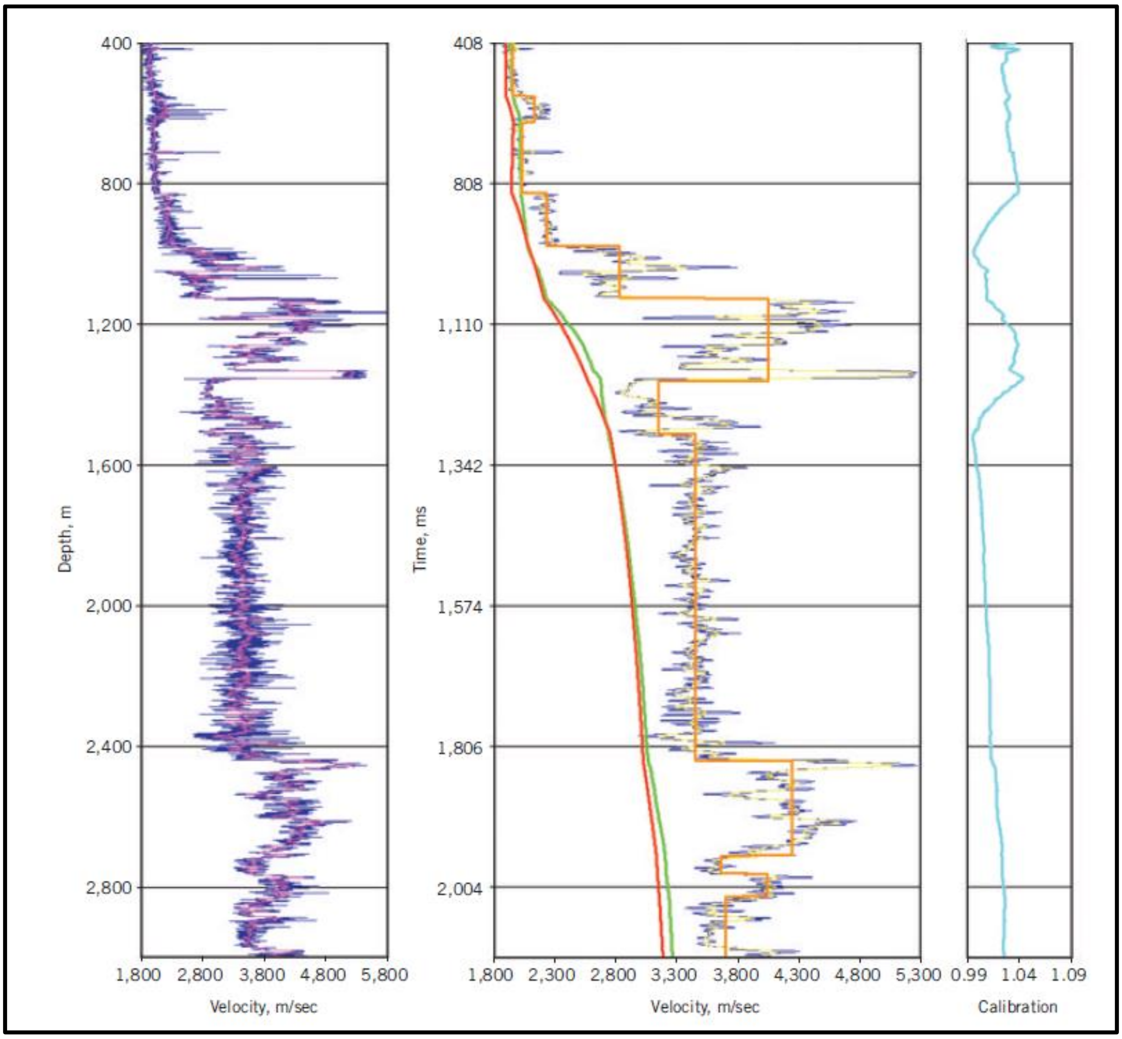

Figure 4.2 Showing velocity calibration (Left, Sonic based raw (blue) and smoothed (pink) velocity logs. The operator length is set to 41 samples, considering average velocity (Vave = 3,500 m/sec), dominant frequency (fd = 35 Hz), and sonic log interval (ISonic = 0.125 m). Sonic based velocity logs, center, as a function of two-way time; subsampled (blue), smoothed (yellow), interval velocity (orange), and average velocity (green). Seismic-based average velocity function (red) from nearest location. Calibration curve, right, is computed from ratio of sonic and seismic average velocity functions.)

Fig. 4.2 shows stepwise transformation of a sonic based velocity log into an average velocity function for comparison with the nearest seismic velocity function to generate a calibration curve. The resolution of the sonic log is about 61 cm or even less, and that of the seismic is 10 m at shallow depths and around 50 m at greater depths. Thus, the seismic resolution is approximately 1⁄100 that of the sonic log. The velocity functions instead have coarse samples of velocity-time pairs picked at prominent reflectors during velocity analysis. The sonic based velocity log resolution is reduced by applying a large length moving average operator. The operator length is computed by considering the seismic resolution and sonic log interval. The average wavelength of seismic data is given by Equation 1, where V_{ave} is average velocity and f_d is dominant frequency, and the seismic resolution is given by Equation 2. The operator length is set to 1⁄10 of seismic resolution and is given by Equation 3, where I_{Sonic} is sonic log interval. The smooth velocity log is then subsampled at 1⁄4 the operator length. The subsampled velocity log is further smoothed by applying an 11-point moving average operator. Integrated travel time (TTI), which is the mean travel time in milliseconds, is derived from the sonic interval transit time Δt. This time is doubled to convert the log from depth domain into two-way time (TWT) domain for comparison with seismic velocity functions. Horizon times are available in the closest seismic velocity function as velocity-time pairs, which are used to compute interval velocity function from the velocity log.

Finally, an average velocity function is computed from the interval velocity function. On the other hand, the closest seismic rms velocity function is also converted into an average velocity function. Both the sonic and seismic average velocity functions are matched, and a calibration curve is generated. Each sample of this curve is computed using Equation 4, where V_{Sonic} and V_{Seis} are the sonic and seismic average velocity samples respectively, at a given time.

$$\lambda = V_{ave} \div f_d \qquad (1)$$
$$R = \lambda \div 4 = V_{ave} \div 4f_d \qquad (2)$$
$$N = 0.1\ (R \div I_{Sonic}) \qquad (3)$$
$$C = V_{Sonic} \div V_{Seis} \qquad (4)$$

This curve is multiplied with all seismic based average velocity functions in the area to calibrate them with respect to the sonic log velocity. It must be noted that usually the seismic velocities are decreased or increased by a fixed percentage through multiplication with a constant correction factor. The calibration curve on the other hand represents a time variant correction factor. These calibration curves are then interpolated at all common depth point (CDP) locations with seismic velocity functions, using geostatistical techniques applied in standard gridding procedures. In this way the calibration is not fixed but varies laterally as well as vertically.

Velocity analysis is carried out in X-Works in which RMS velocities are converted into interval and average velocities. Dix equation is used to convert RMS velocity into interval velocity. X-Works uses a velocity processing engine which automatically converts the input RMS velocities into interval velocity and average velocity for time to depth conversion (Khan and Akhtar, 2011).\

4.2.3 loading of data in X-Works

After completion of calibration next step is to load the seismic data and geological cross section onto the X-Works main screen. First step is to load the georeferenced image of seismic and then make the geological model using the same interpretation done on seismic. After that load the calibrated velocity data.

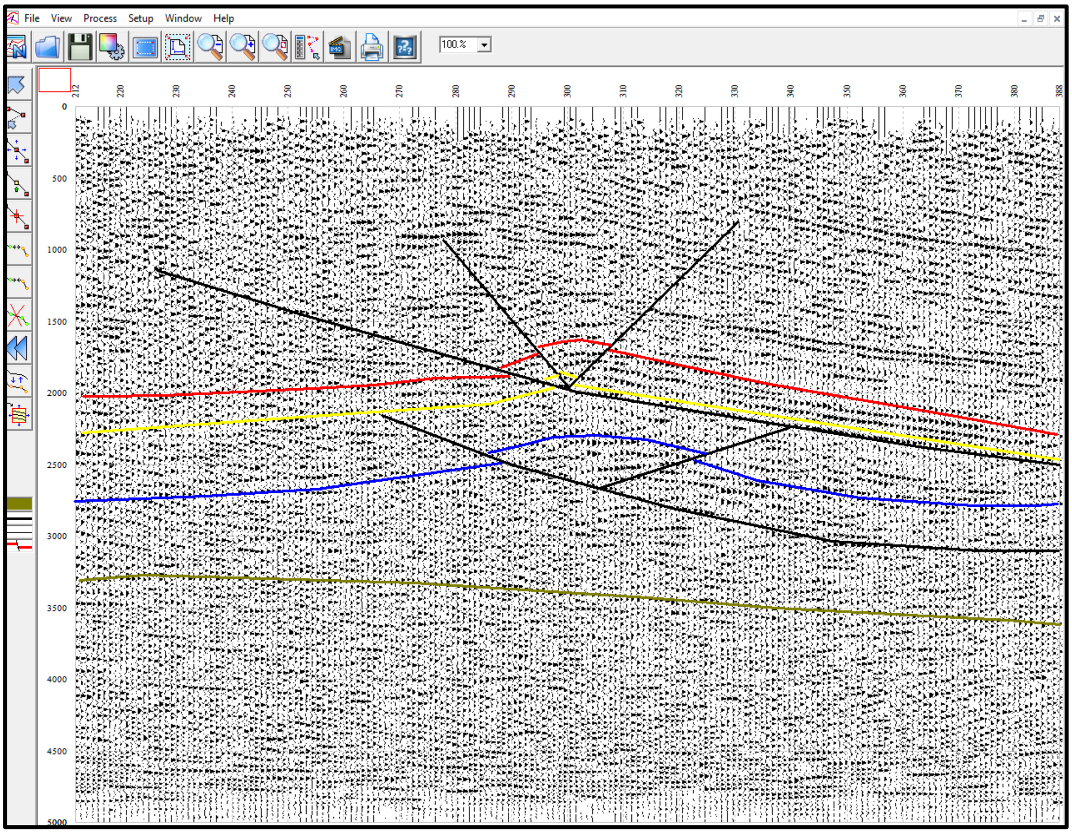

Fig 4.3 Seismic section with geological model on X-Works

When velocity function is loaded into the program all the three velocity types are loaded in correspondence with the CDPs i.e., Interval velocity, RMS velocity and Average Velocity.

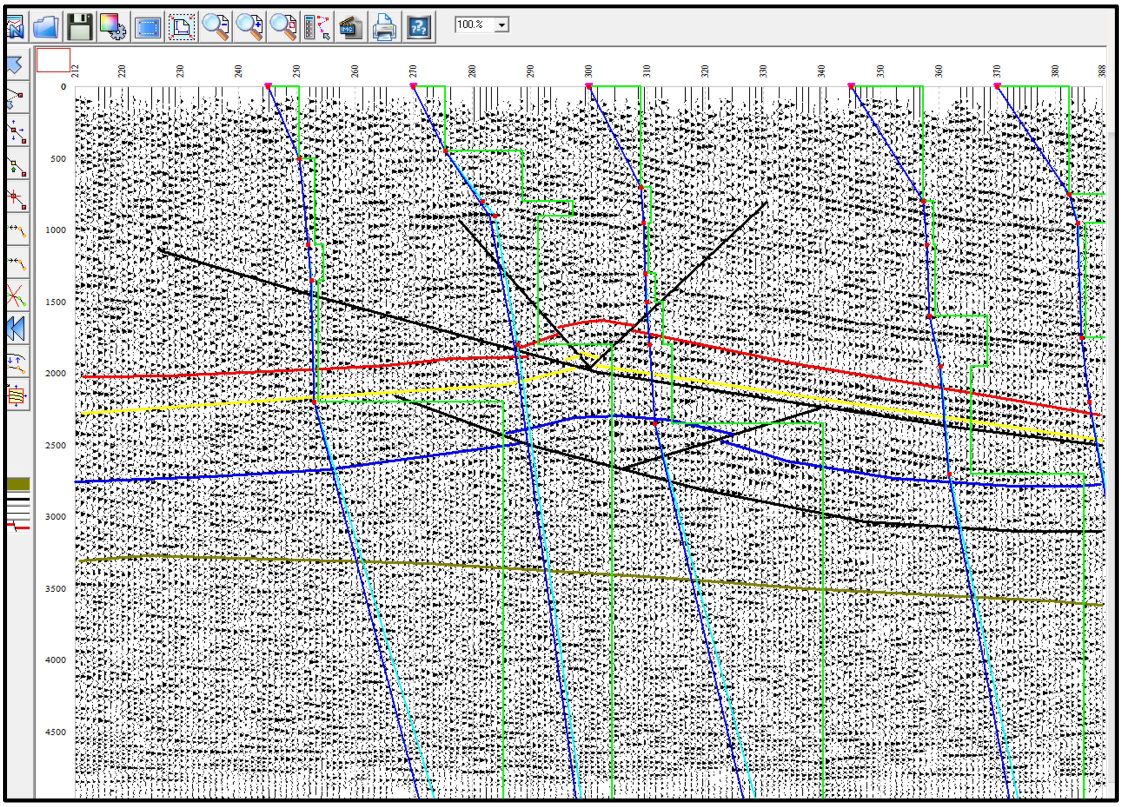

Fig 4.4 Interpreted seismic section with Velocity data (RMS, Interval, Average)

4.2.4 Spatio-Temporal Interpolation

Spatio means space, velocity analysis is carried out after intervals after every 50 CDP intervals or looking at the geological structure so we have to interpolate velocity at every CDP or every 10th CDP, this will help us interpolate velocity function in lateral space. Temporal means time because the vertical component of seismic is time so must interpolate velocity vertically. At the end there would have a matrix of velocity that if we have given CDP interval of 10 CDP and vertical interval of 2msec than we would have velocity function at every 10th CDP and vertically 2msec. So, we would have velocity time pairs at every 2msec. In this way we have generated a grid of velocity. Reason to make this grid is we need to apply smoothing to this grid as our velocity may have some artifacts or kinks on basis of noise. For that we apply a 2D moving average for smoothing of velocity it will act as a high cut filter and smooth the velocity

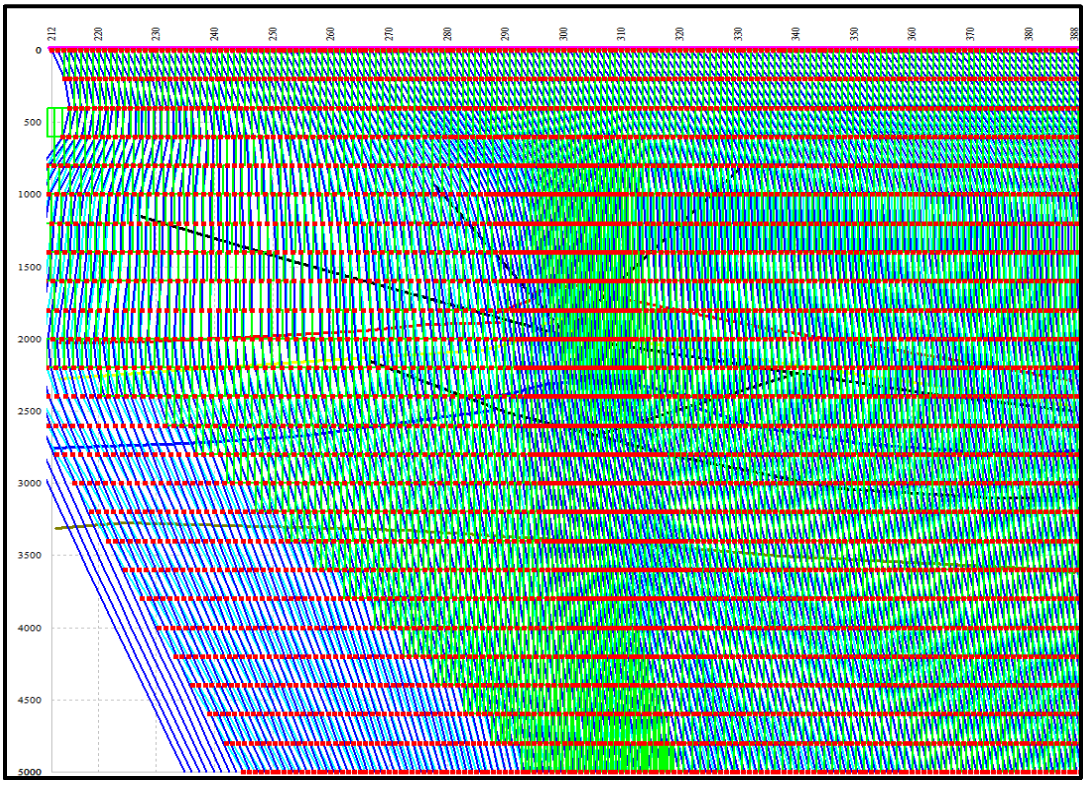

fig 4.5 Interpolated velocities at 200ms interval (red) RMS, (green) Interval, (Blue) Average

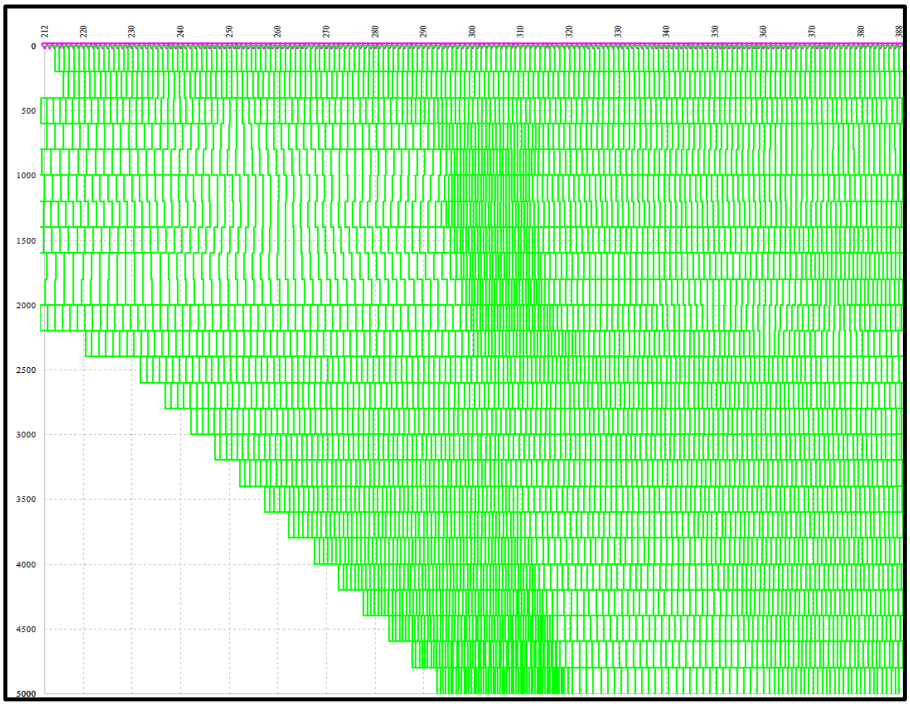

Figure 4.6 Interpolated Interval velocities at 200ms interval

4.2.5 Horizon Velocity Interpolation

After the interpolation of velocity, next step is inputting the seismic interpretation which include the horizons and faults and then will interpolate the velocity with them. Now based on the horizon and faults the velocity functions that have previously gridded they would interpolated on basis of seismic interpretation, computing them will give us interval-based velocity model that will be a real velocity model. The word real is used because velocity is changing according to the geological structure and in other words, It can be said that it is a subsurface image in terms of velocity.

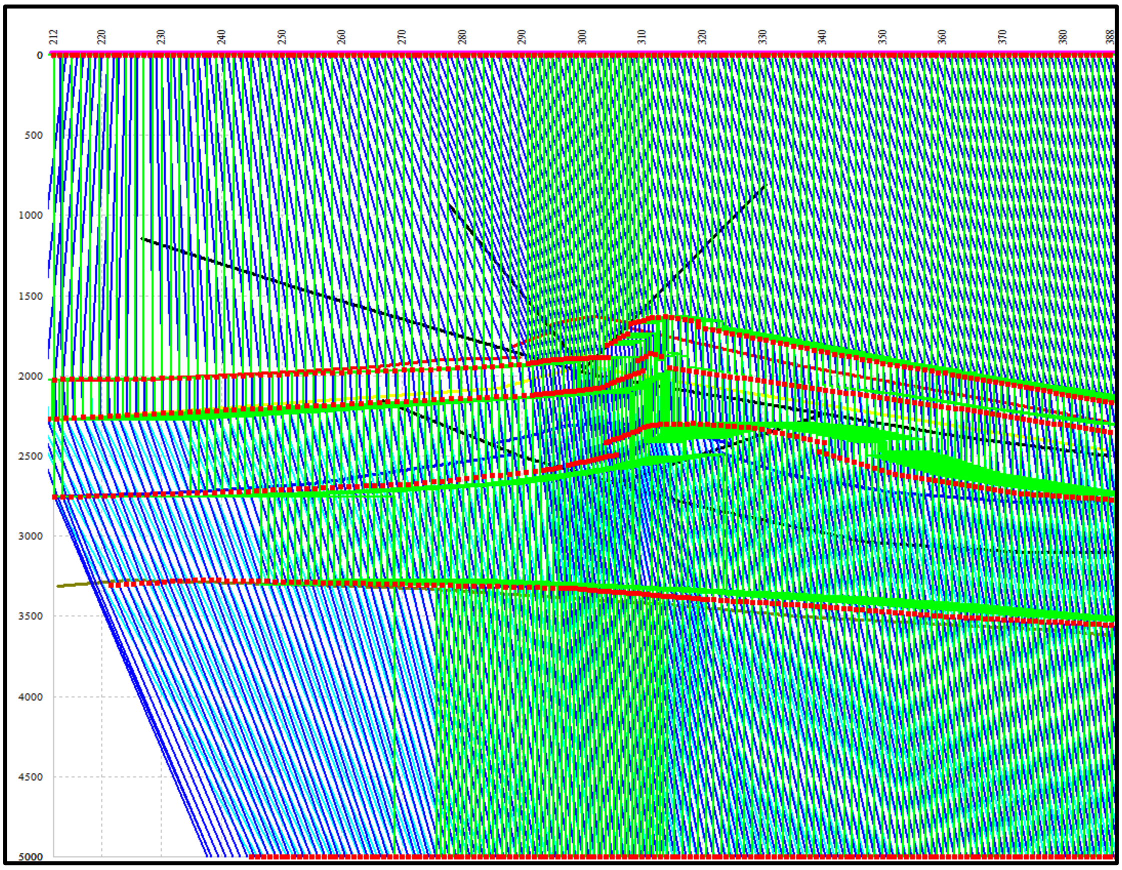

Figure 4.7 Horizon interpolated velocities (Velocity model) at 200ms interval (red) RMS, (green) Interval, (Blue) Average

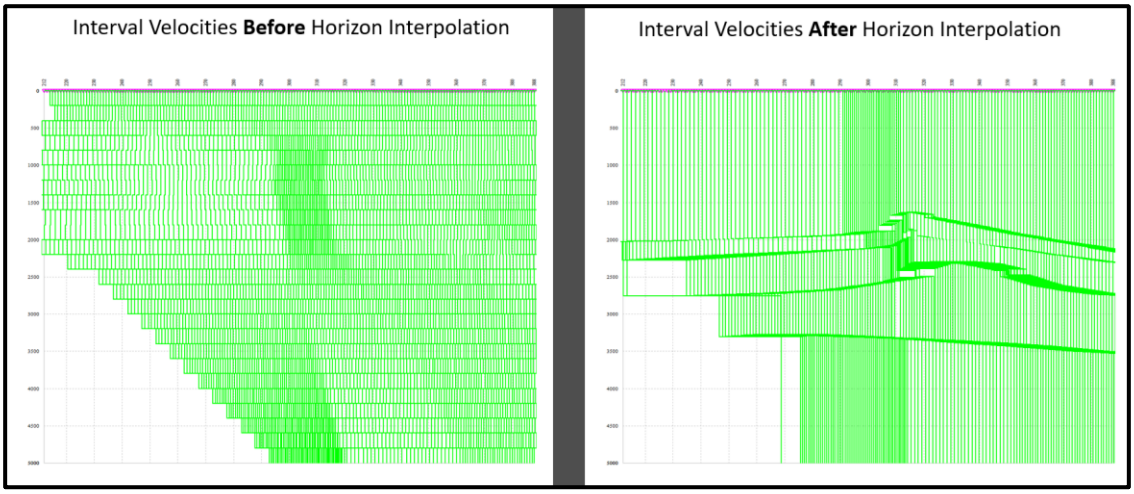

Figure 4.8 Before and after in change in velocities from Horizon based Interpolation

The figure 4.7 and figure 4.8 above are showing the final velocity model generated which are giving us more realistic velocities of the subsurface. These velocity models are very helpful they can help us in various applications of geophysics for example this velocity can be used to generate depth contour maps and a major application is post-Stack depth migration.

4.3 2D SEISMIC MODEL

2D forward modelling will help us in validating our previously generated velocity model. To generate a 2D Forward model one must convolve the horizon interpolated velocity model with a source wavelet generated through seismic and that will give us a synthetic section based on 200 msec interval. This synthetic seismic section will show me more matching to geological subsurface information on contrary to synthetic section generated with velocities that were not interpolated with horizons.

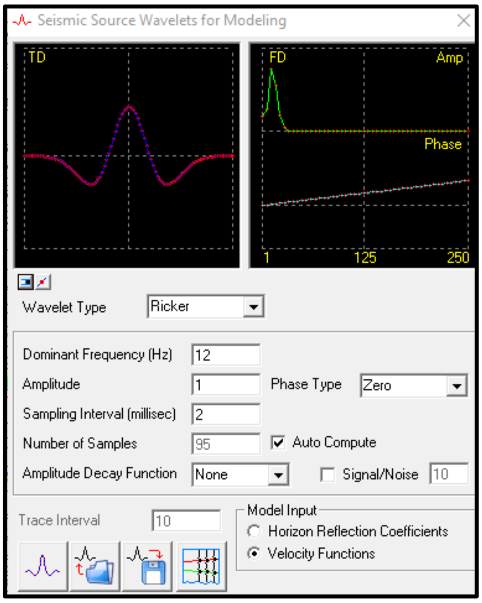

Figure 4.9 Ricker wavelet generated at 12Hz sweep frequency to convolve

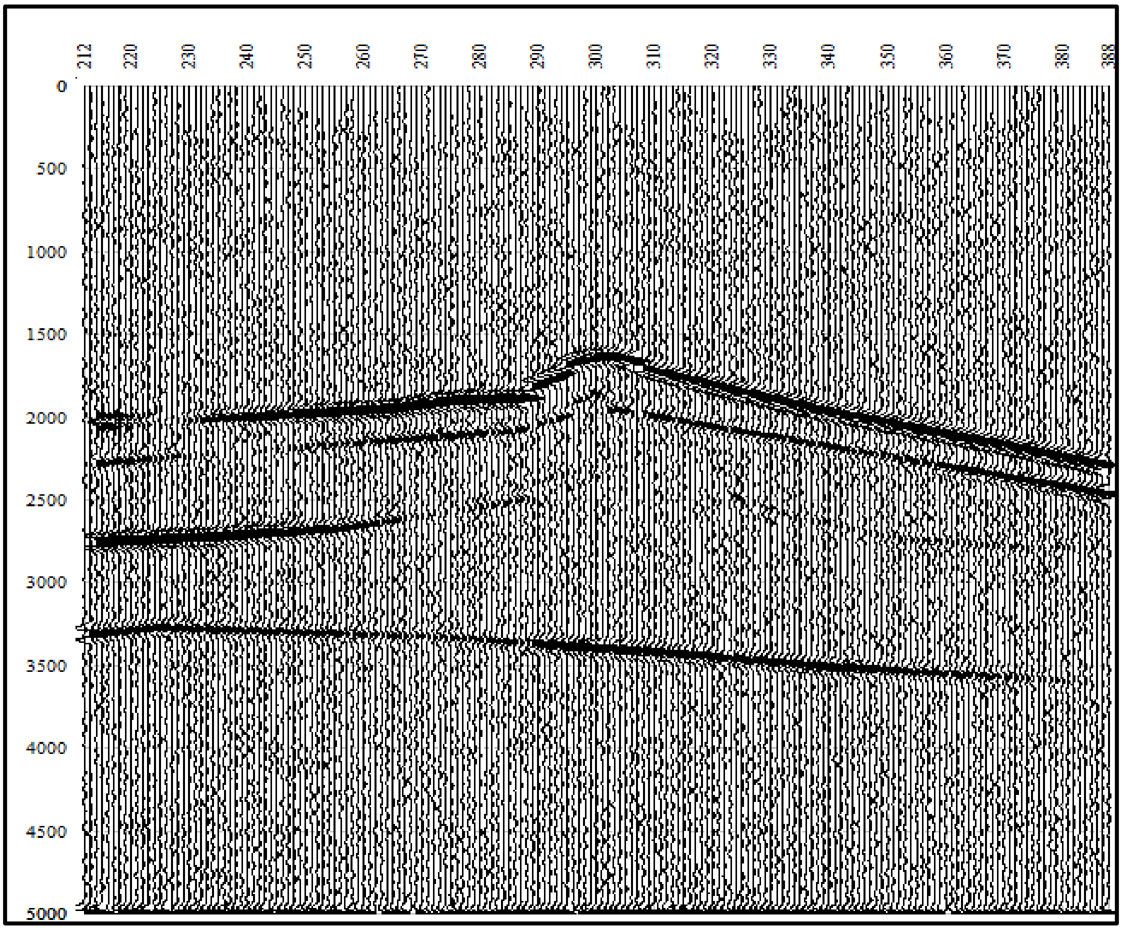

Figure 4.10 2D Seismic Model of Interpreted Geologic section of Line 884-FMK-107

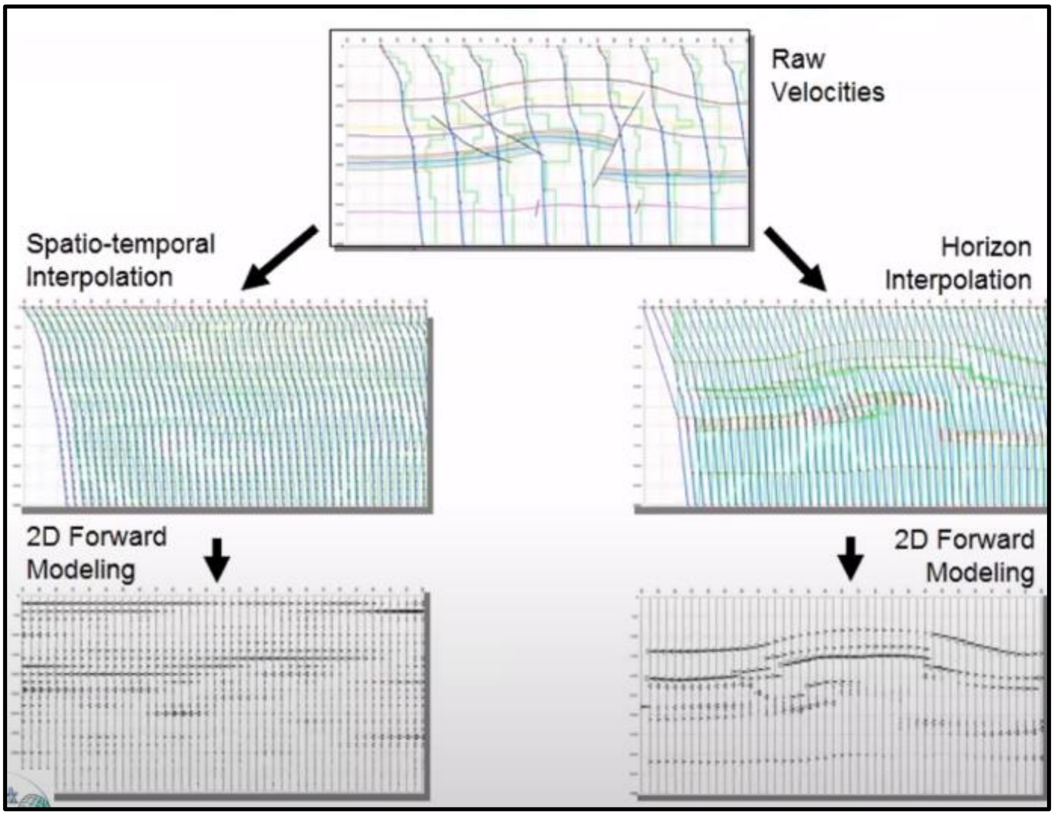

Figure 4.11 It difference synthetic model generated without and with horizon Interpolation

Figure 4.11 demonstrate how horizon interpolation help us in generating a true 2D seismic model which matches more with the real geological Information on contrary to model generated with only spatio-temporal interpolated model.

CHAPTER 5

POST STACK PROCESSING

5.1 INTRODUCTION

Reference of our working on available six seismic lines, both lateral and vertical velocity change has been noted along the lines. The post stack processing was considered for overall improvement in signal to noise ratio, imaging, resolution and to help for more confident interpretation of faults and horizons. Seismic line 884-FMK-107 was selected for post stack processing. The post stack processing sequence has been described in subsequent paragraphs.

The Seismic and well data is provided by Directorate General of Petroleum Concessions, Pakistan (DGPC) Islamabad, Pakistan. The provided 2D seismic line is un-migrated, SEG-Y format. Processing software is used for the migration of un-migrated seismic data. Already generated velocity model was used for post stack depth and time migration.

5.2 IMPLICIT FD TIME MIGRATION

Implicit FD Time Migration performs a post stack time migration using a Finite Difference algorithm capable of improved accuracy at steep dips. This migration is carried out in depth, time and frequency domains so that the input stack is converted in to frequency domains. The improved response at steep dips results from the use of a special form of the higher order approximations to the dispersion relation. The six levels of approximation included in the program are referred to as 15, 45, 45, 80, 87, and 90 degrees.

As indicated above, this process provides a time migration, not a depth migration. However, the velocity field is allowed to vary as a function of both coordinates, and, within the limitations of a time migration, the process will accurately migrate and focus events in a spatially varying velocity field. Internally, the migration algorithm uses interval velocity as a function of time.

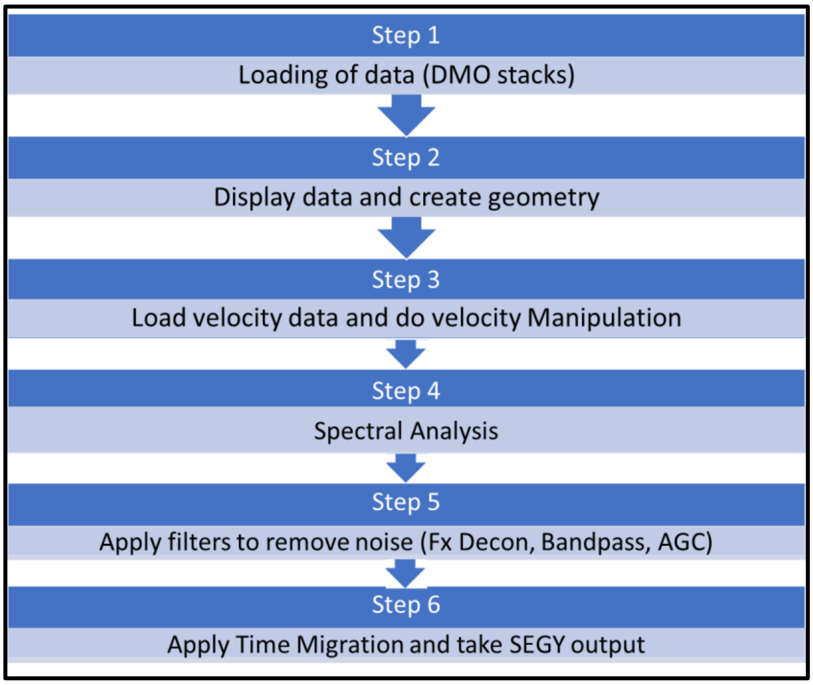

Figure 5.1 Flow chart explaining all steps involved in time migration

The procedure adopted for processing for Implicit FD Time Migration is as follows.

5.2.1 Step 1 - Load stack data

1) Make new project.

2) Make new Line

3) Make a new flow

4) Read SEG-Y stack data.

5) Seg-y input parameters are displayed in figure 5.2

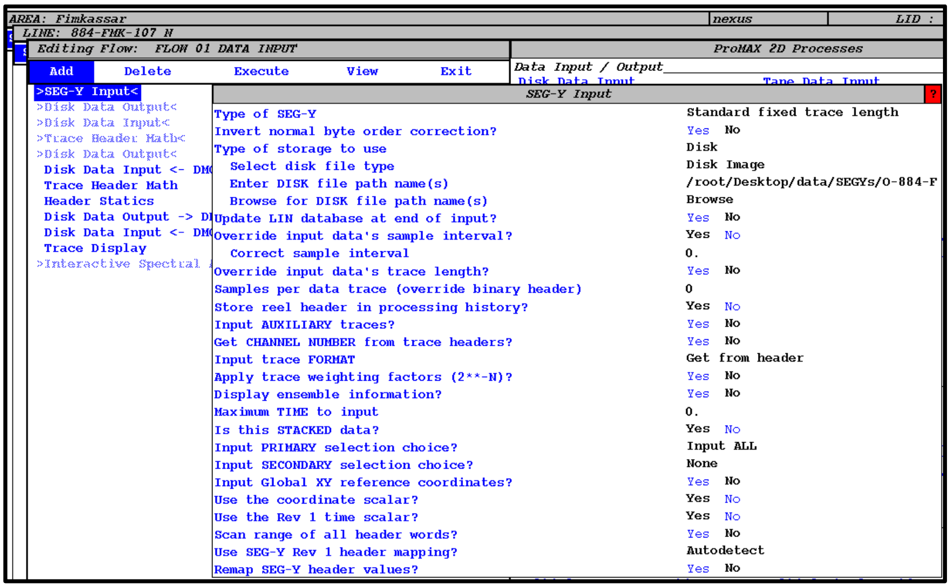

Figure 5.2 SEG-Y input parameters

1) Generate Disk data output (SEG-Y data saved in ProMAX internal format).

2) Disk data output parameters are listed in figure 4.2

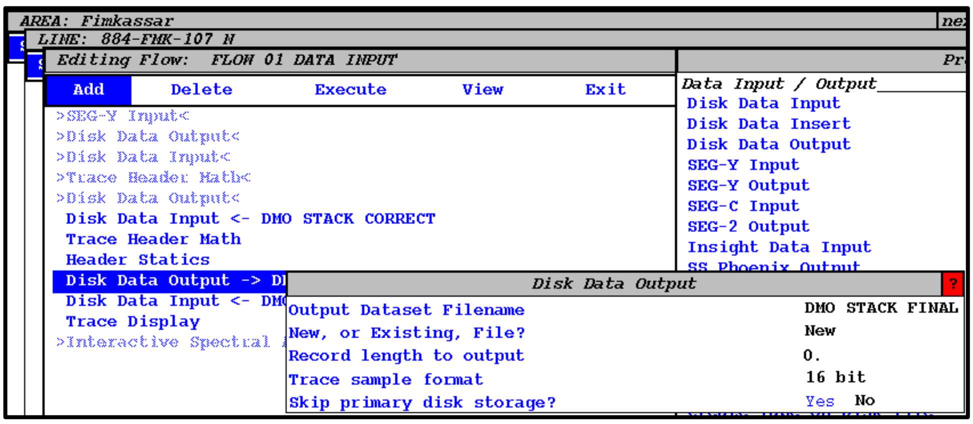

Figure 5.3 SEG-Y output parameters

5.2.2 Step 2 - Display stack data

1) Make a new flow for data display

2) Set Input parameters in disk data input.

3) Add trace display module for display.

4) Run trace display flow.

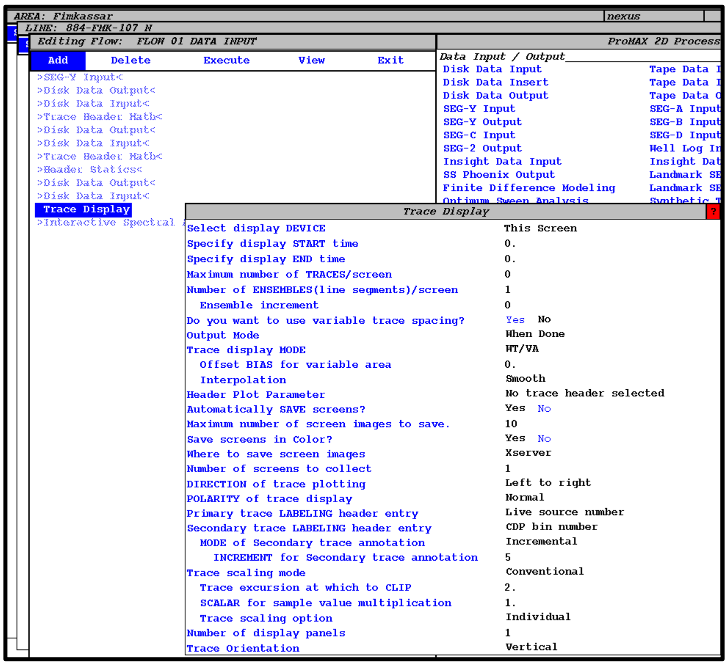

Figure 5.4 Display flow window

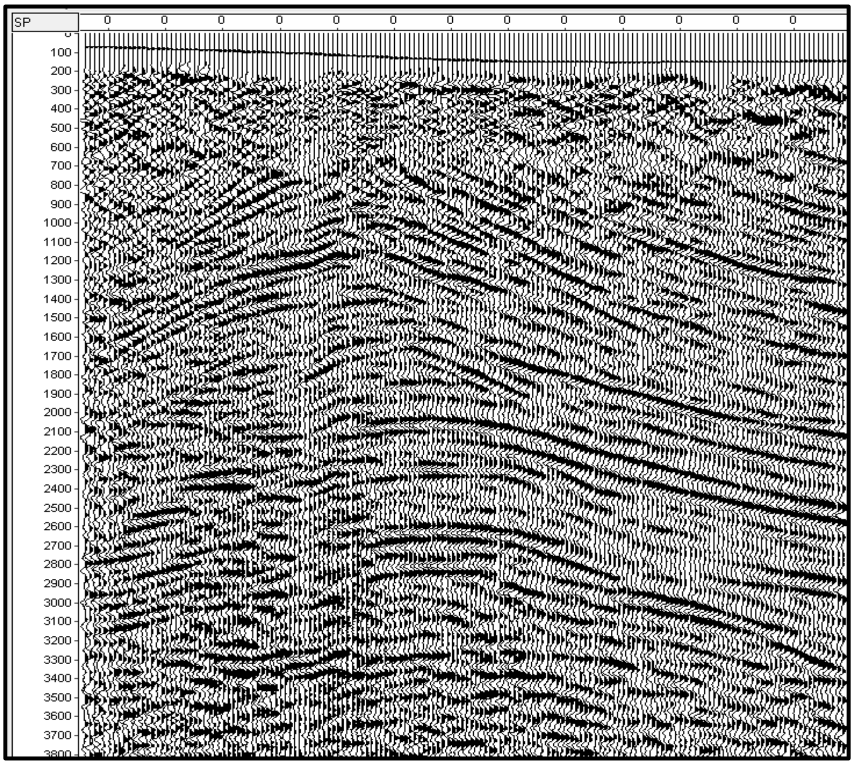

Fig 5.5 DMO unmigrated stack display 884-FMK-107

5.2.3 Step 3 - Create CDP database

Add another flow to create CDP database geometry. The first and last CDP and stations set for further processing flows.

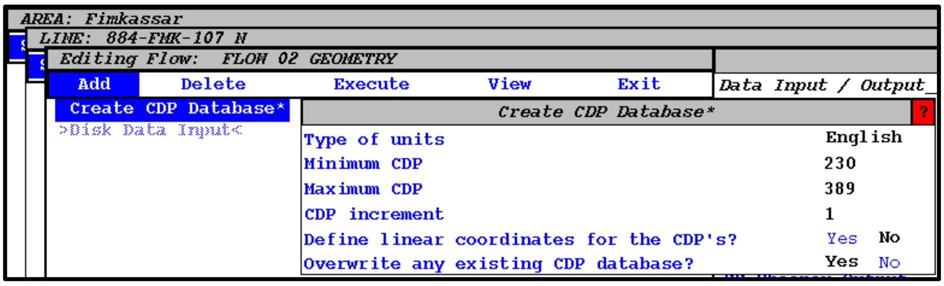

Fig 5.6 Flow for CDP database

5.2.4 Step 4 - Input stacking (rms) velocity

Create another flow for velocity manipulation. Add two modules for view, smoothing, velocity conversion from rms to interval velocity and quality control of converted velocities in velocity viewpoint editor.

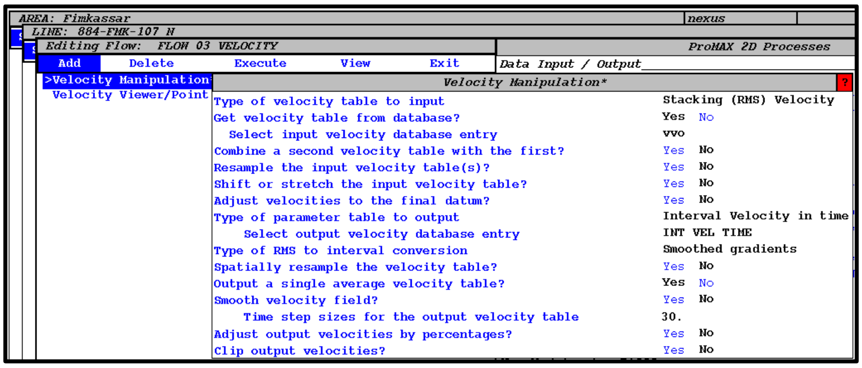

Fig 5.7 Flow for velocity manipulation

1) Volume view editor (Import velocities from work done on X-works software for velocity modelling on line 884-FMK-107 as already explained in chapter 6

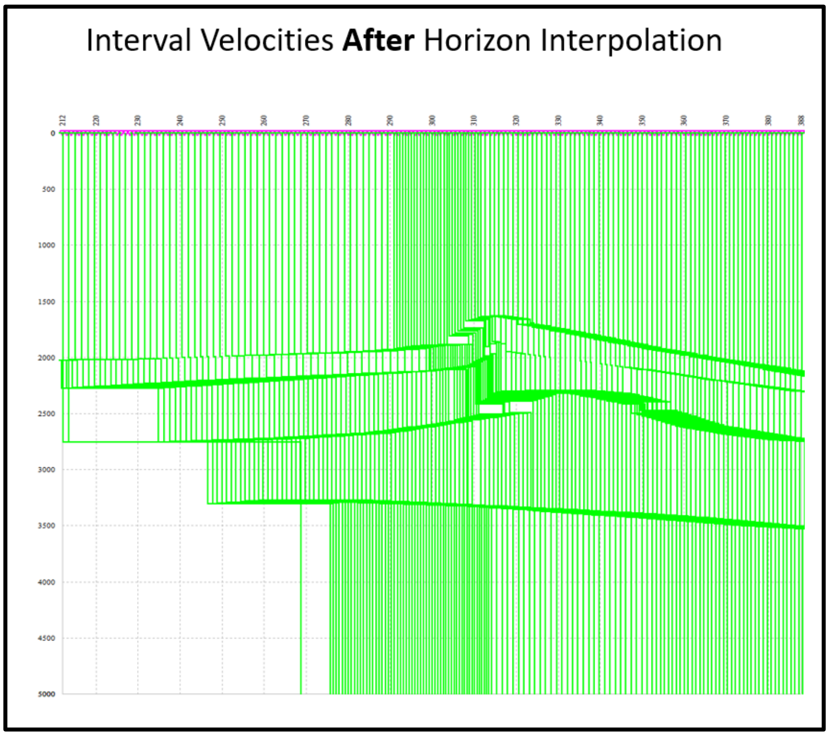

Fig 5.8 Interpolated Interval velocity model generated and displayed in X-works software

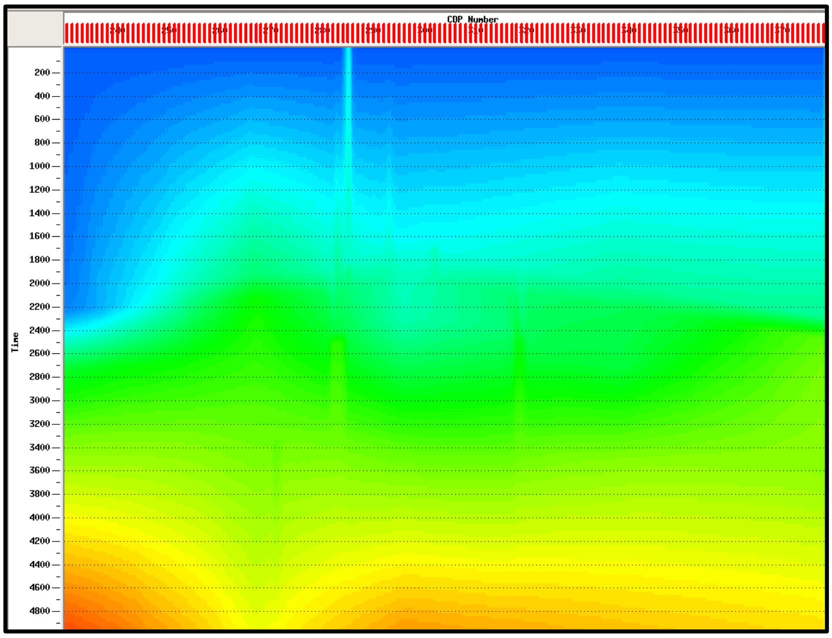

Fig 5.9 x-works Interval velocity in time displayed in ProMAX

5.2.5 Step 5 - Display edit/smooth rms velocity

Open table from velocity viewer editor from step 4, create a new output table for smoothed velocities. The smoothing parameters are as under

1) New CDP smoothing interval = every 20 cdps
2) Time smoothing interval = 200 milli second
3) Horizontal Smoothing operator length = 40 cdps
4) Vertical smoothing operator length = 500 ms
5) imported in promax
6) Smooth velocity (interval velocity in time)

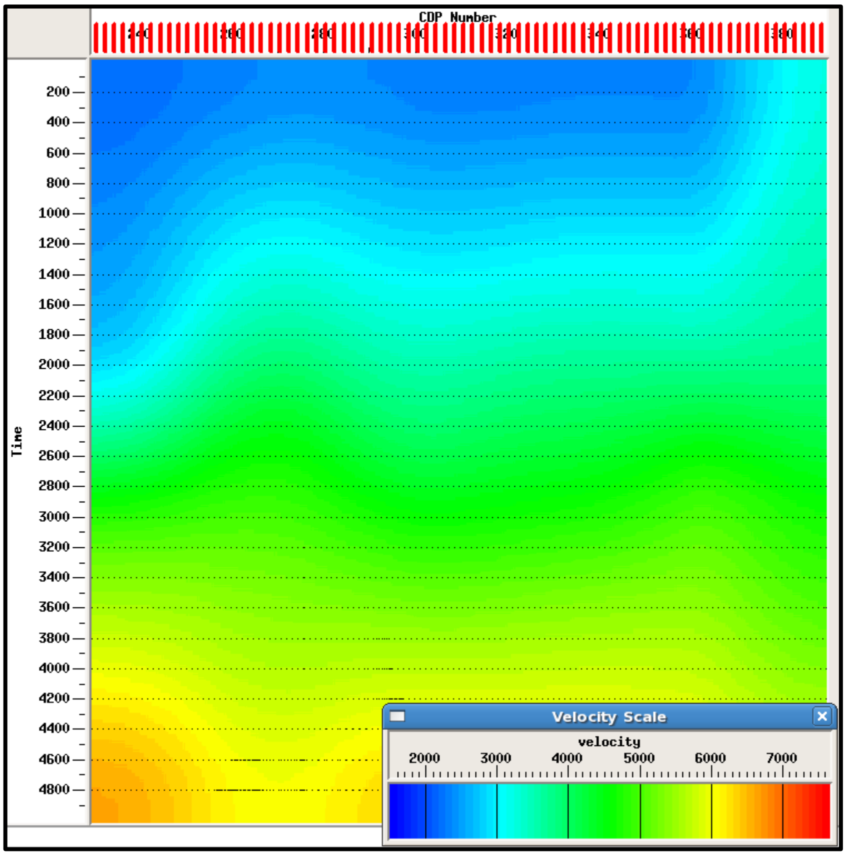

Figure 5.10 Smooth Interval in time velocity in ProMAX

5.2.6 Step 6 - Convert time interval velocity into depth interval velocity

Input smoothed time interval velocity table from above step in velocity manipulation module, add output velocity table name for depth interval velocities. Velocity manipulation module use DIX equation module to convert time interval velocity to depth interval velocities both in depth and time.

Display interval velocity table using velocity viewpoint editor module as in figure

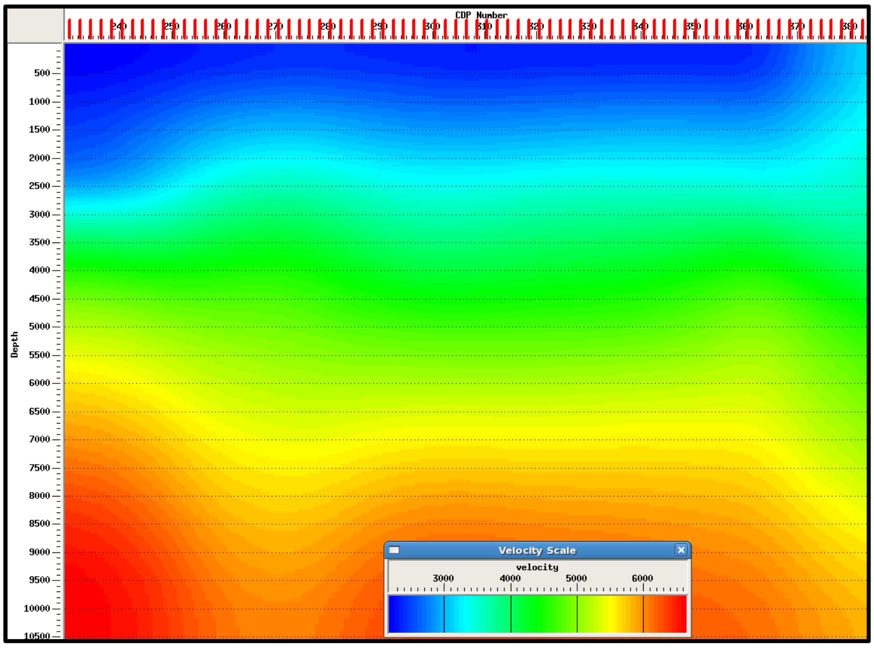

Fig 5.11 Time interval velocity converted to depth interval velocity

5.2.7 Step 7 – Post-stack processing/signal enhancement parameter testing

1) Spectral analysis

Using ProMAX spectral analysis module to view the minimum/maximum frequency range of data, read the spectrum value down to -20db. This analysis help in selection of band pass filter range.

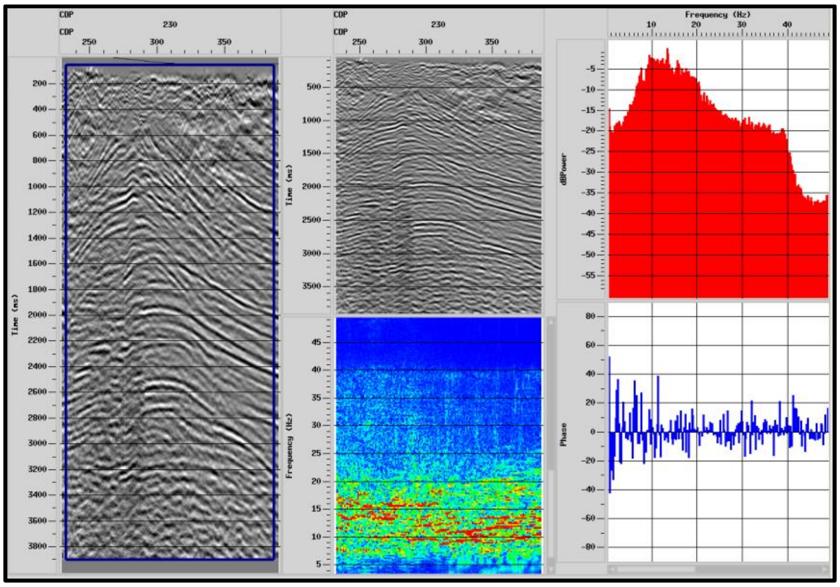

Fig 5.12 Display of spectral analysis of complete stack

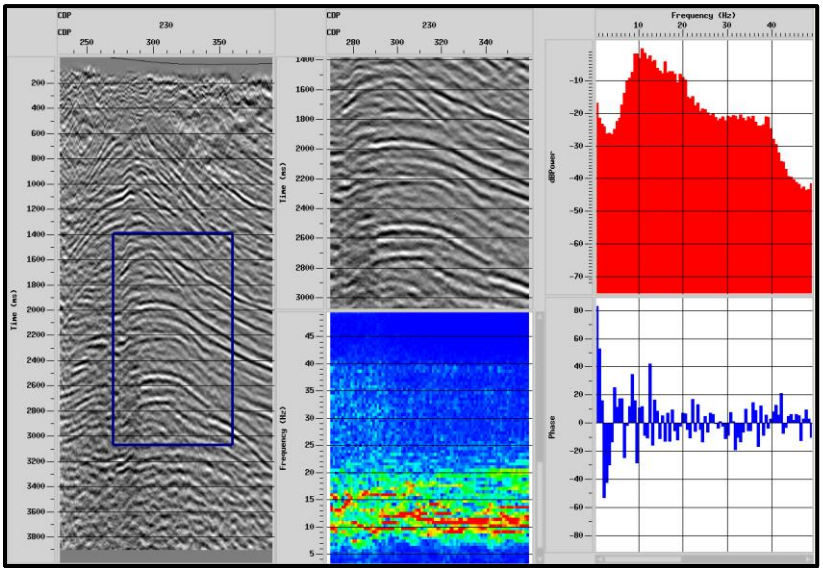

Fig 5.13 Display of spectral analysis of zone of interest

2) Band Pass Filter

To remove the unwanted noise effects from the seismic data for a frequency interval, band pass frequency filtering is used. To use a bandpass filter, the frequency range of the data must be decided. So that, unwanted low and high frequency can be removed from the data. Foremost, wanted frequency interval is remained to be processed (Uygun, 2016).

Bandpass Filter applies a frequency filter(s) to each input trace. Data should be bandpass filtered before migration to avoid artefacts caused by abruptly truncating the frequency band.

1) Pass band: 8-44 Hz
2) Low cut: 4-8 Hz
3) High cut: 44-48 Hz
4) BP filter: (4-8-44-48) Hz

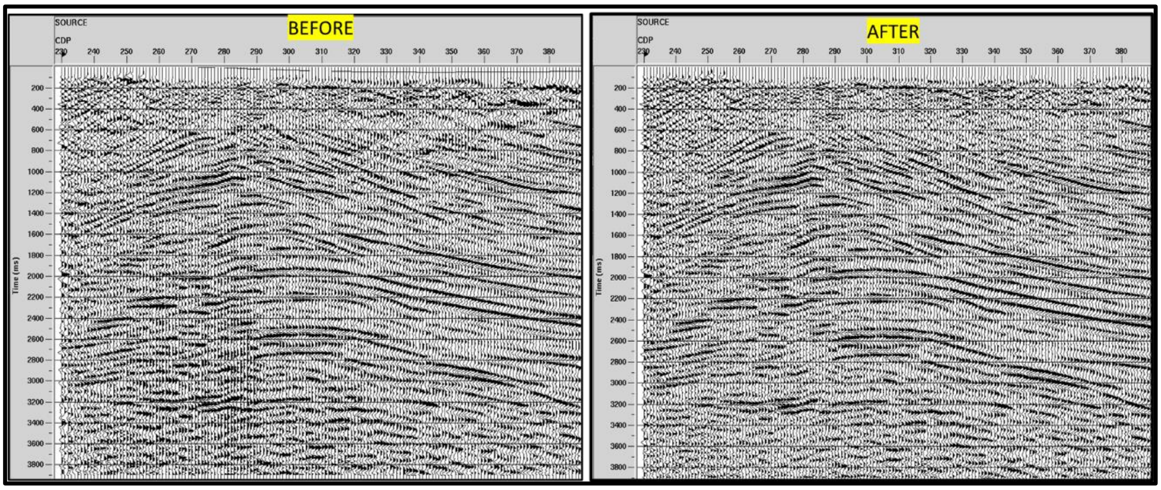

Fig 5.14 Before and after stack applied band pass filter

Now as in fig 5.14 it is seen that reflectors are more pronounced as compared to before filtering especially in deeper parts of data a lot of unwanted noise is removed and stack looks more refine

3) Random noise attenuation

F-X Deconvolution applies a Fourier transform to each trace of an input ensemble or stacked data. It applies a complex, Wiener, unit prediction filter in distance for each frequency in a specified range, and then inverse transforms each resulting frequency trace back to the time domain. This process produces output with less random noise than the input data (Treitel, 1974).

F-X Deconvolution was applied to the stack data for random noise attenuation this process produces output with less random noise than input data as shown in figure.

1) Horizontal window: 11 cdps
2) Vertical window: 1000 ms
3) Window overlap: 200m
4) Min/max frequency: 4-48 Hz

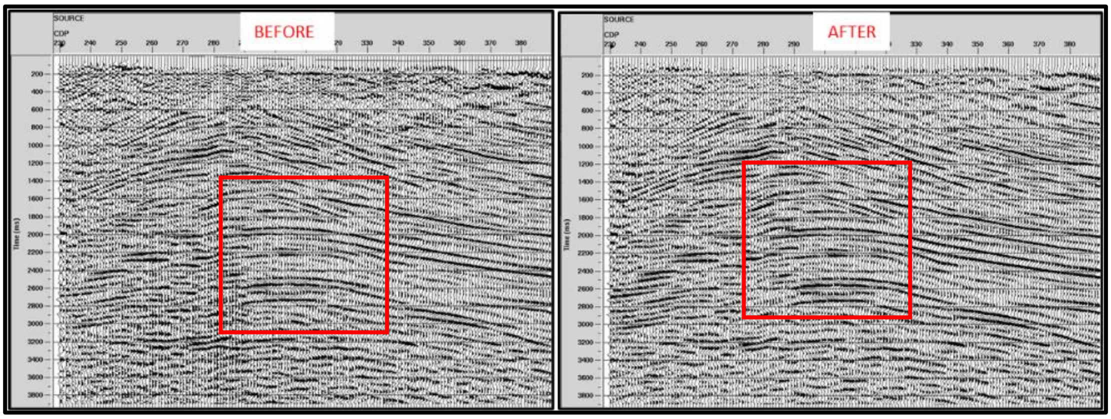

Fig 5.15 Before and after stack applied FX Decon filter

The highlighted red boxes in fig 5.15 shows that how random noise was removed using the FX-Decon filters and prominent reflectors are more pronounced.

4) Automatic Gain Control (AGC)

Automatic gain control (AGC) is one of the most common gain recovery methods in seismic processing. AGC is applied to the seismic data on a trace-by-trace basis using a sliding time window. AGC is used in data processing to improve the visibility of seismic data in which attenuation or spherical divergence has caused amplitude decay (Dondurur et al., 2018).

AGC automatically varies the gain applied to trace samples as a function of sample amplitude within an AGC time window(750ms).

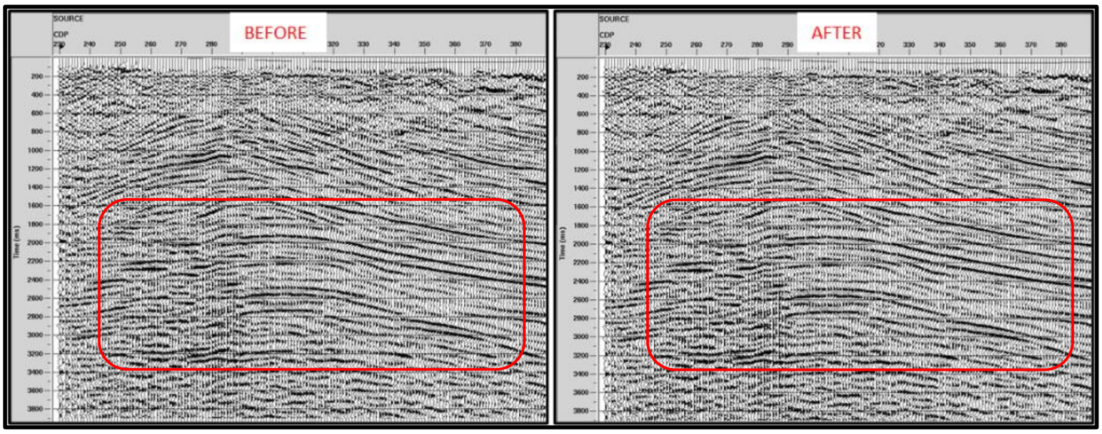

Fig 5.16 Before and after stack applied AGC

You can notice that the energy is not visible in some of the record on the left of Figure 5.16. AGC applied approximately removes the loss of energy (spherical divergence) and equalized the amplitudes with improved resolution (on the right). AGC makes all events visible and appear balance in the data

5.2.8 Step 8 – Migration parameter testing

Input un-migrated stack data, Apply above post stack processing at step 7. Run implicit FD time migration with 90%,100% and 80% scaled velocities.90% scaled velocity proved to be the appropriate for properly migrating data from top to bottom level as shown in figure 4.8

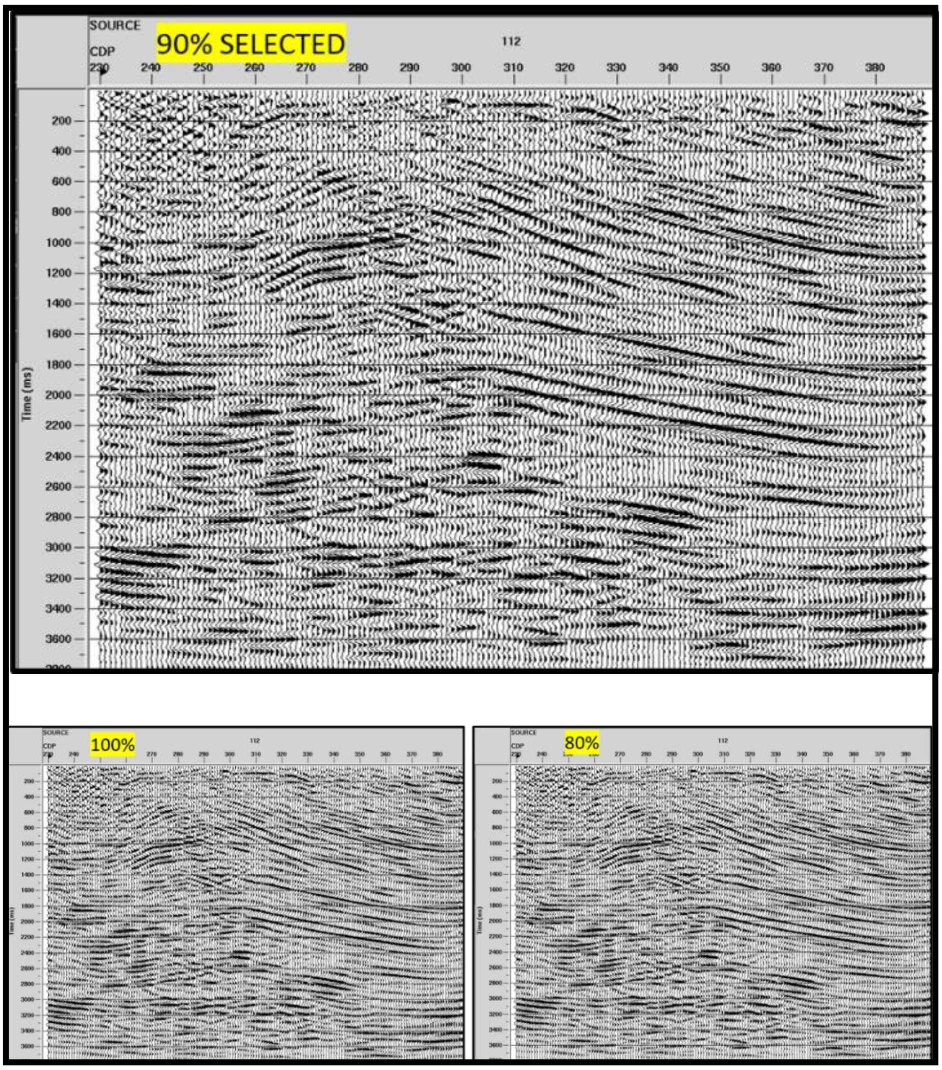

Figure 5.16 Implicit FD time migration with 100%,90% and 80% scaled velocities on line 884-FMK-107

5.2.9 Step-9 Post-Stack Migration flow

1) Disk data input: Un-Migrated stack section
2) Band pass filter
3) F-X decon filter
4) AGC (Automatic Gain Control)
5) Implicit FD Time Migration (using 90% velocities)
6) Disk Data output (Migrated stack section)

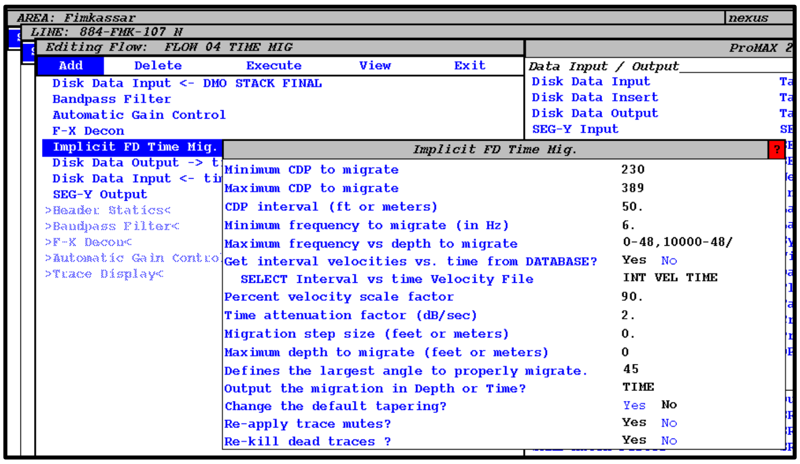

Figure 5.17 Post stack migration flow

5.2.10 Step 10 – Display and seg-y output and display

Display all stacks on screen for Screen captures for presentation and overall result quality control. Output all migrated stack into SEG-Y output format for interpretation.

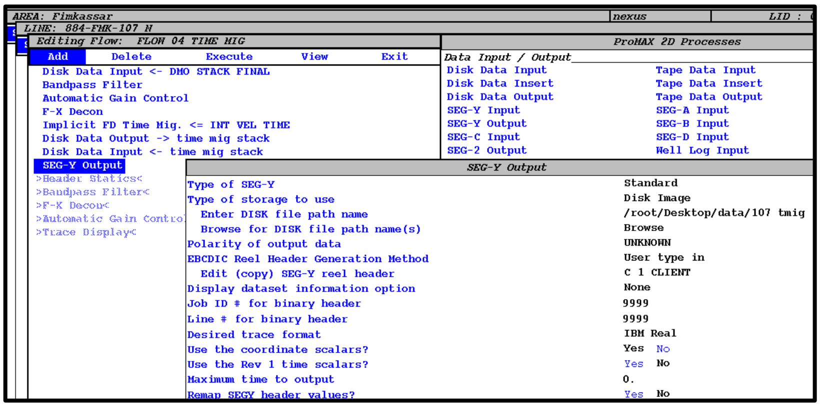

Fig 5.18 flow for SEGY output of migrated stack

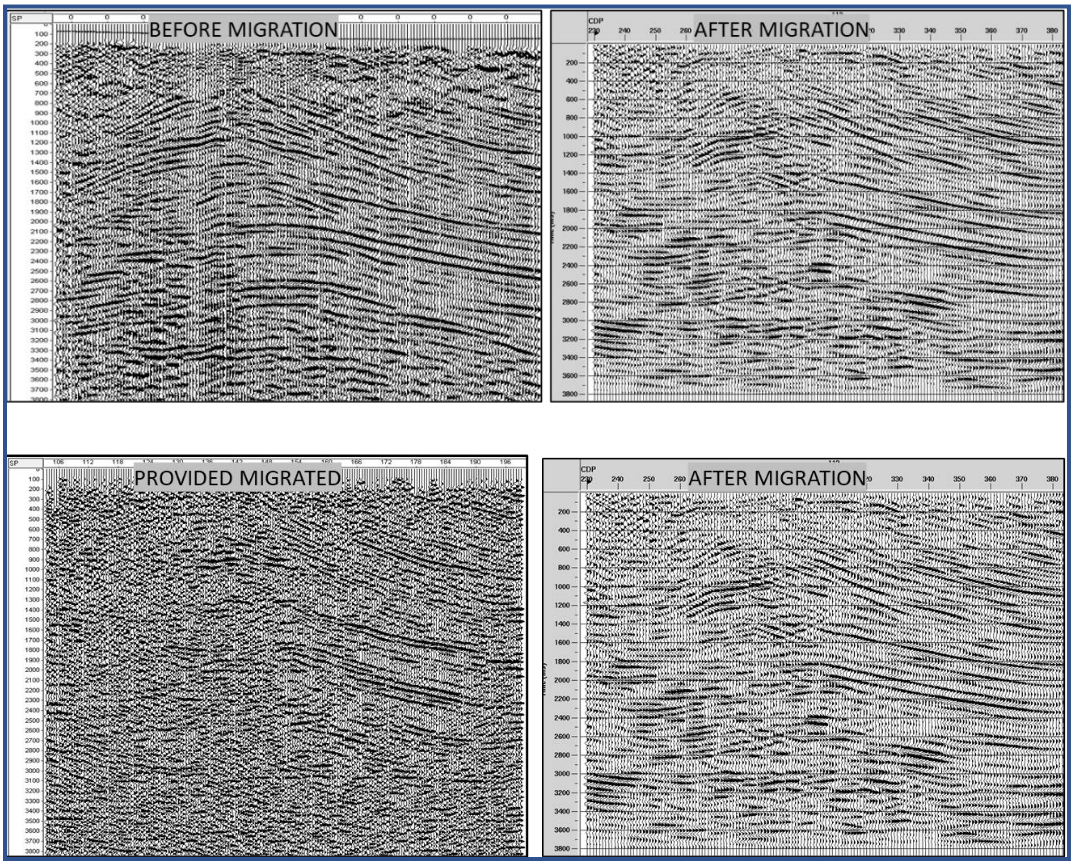

Figure 5.19 Line 884-FMK-107 before and after migration.

The fig 5.19 shows us the final migrated section as well as provided migrated and un-migrated sections. It is clearly visible from the above images that processing parameters helped us a lot with interpolated velocity model to form a section that has less energy loss in terms of amplitude with much more visible reflectors and less noise if compared to un migrated section.

5.3 IMPLICIT FD DEPTH MIGRATION

Implicit FD Depth Migration performs a post stack depth migration using a Finite Difference algorithm capable of improved accuracy at steep dips. This migration is carried out in depth, time, space, and frequency domains so that the input stack is converted from time to frequency domains.

The improved response at steep dips results from the use of a special form of the higher order approximations to the dispersion relation. The six levels of approximation included in the program are referred to as 15, 45, 65, 80, 87, and 90 degrees. Internally, the migration algorithm uses interval velocity as a function of depth.

The reliability and accuracy of the results of any depth migration are highly dependent upon the quality of the velocity model used to migrate the data.

5.3.1 Step 1 Post Stack Depth Migration

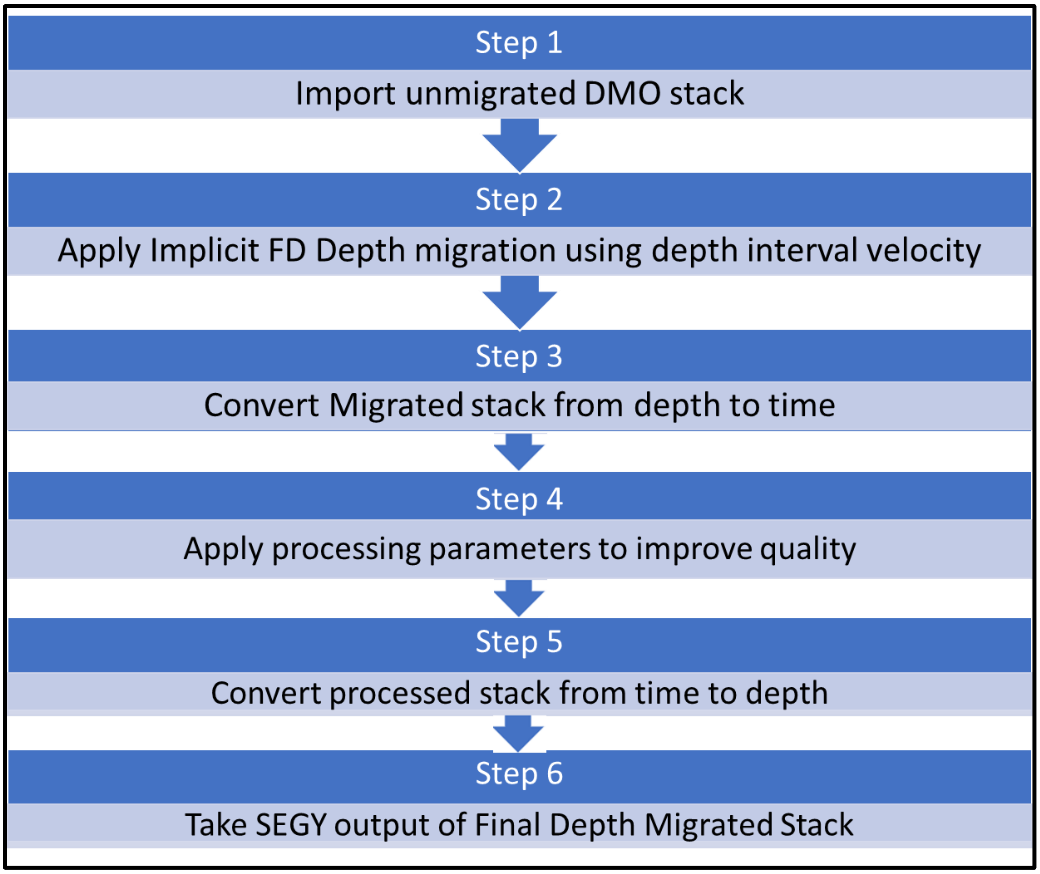

Figure 5.20 Flow including steps involved in Depth Migration

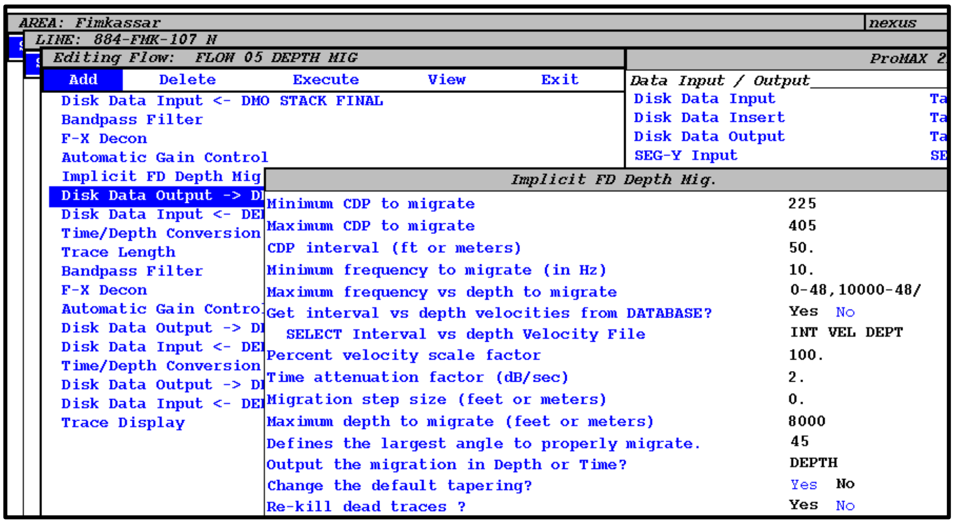

Figure 5.21 processing flow for depth migration

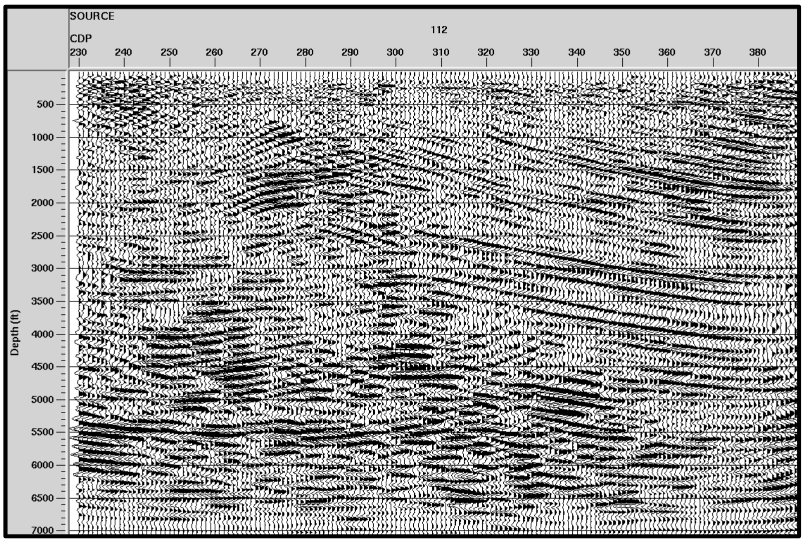

Figure 5.22 Initial Depth migrated stack

5.3.2 Step 2 Depth to time conversion

In this step depth migrated stack will be converted to time section. The reason behind converting the section to time so processor can apply processing to enhance the resolution of stack and remove noises as filtering can only be applied to time section

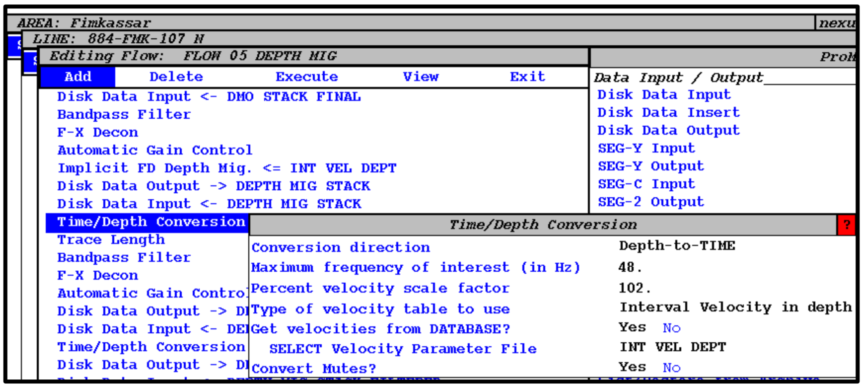

Fig 5.23 Flow for depth to time conversion

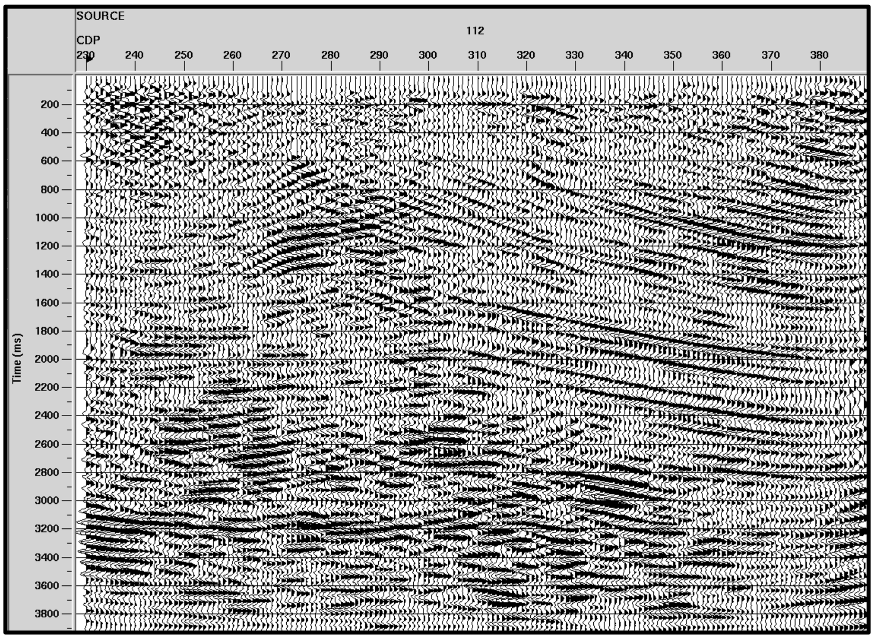

Figure 5.24 Depth to time converted stack

Once the section is converted to time as in figure 5.24 than next step is applied filters including Band Pass, FX Decon and AGC to enhance the section to produce a output shown in figure 5.25

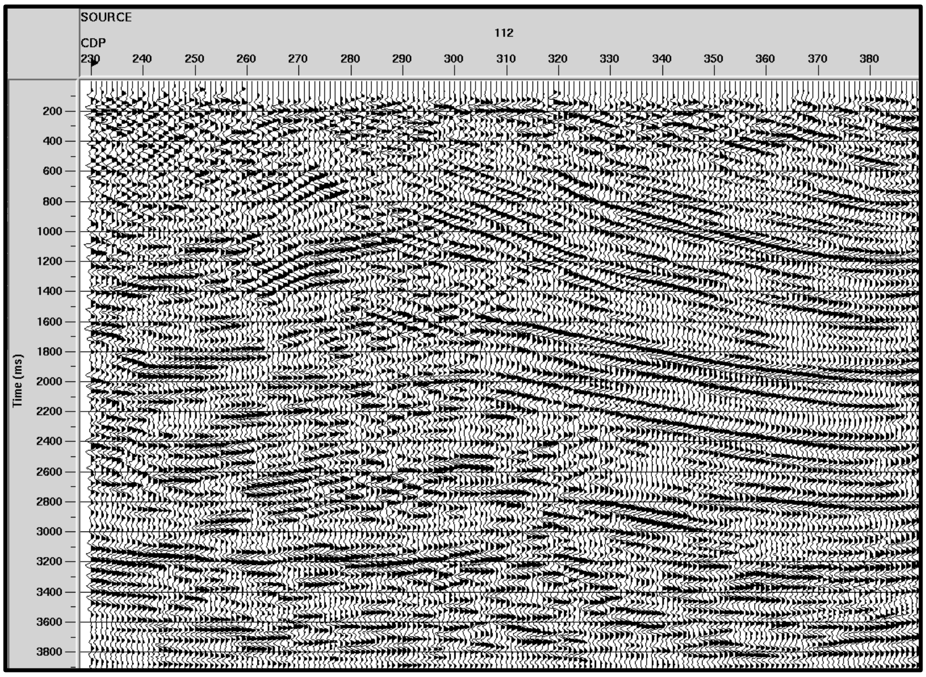

Figure 5.25 Depth to time converted stack with all post processing done

5.3.3 Step 3 time to depth conversion

After applying filters on time converted section next step is to convert it back to depth so a new flow for depth conversion will be made and final depth migrated stack will be generated as displayed in figure 5.27

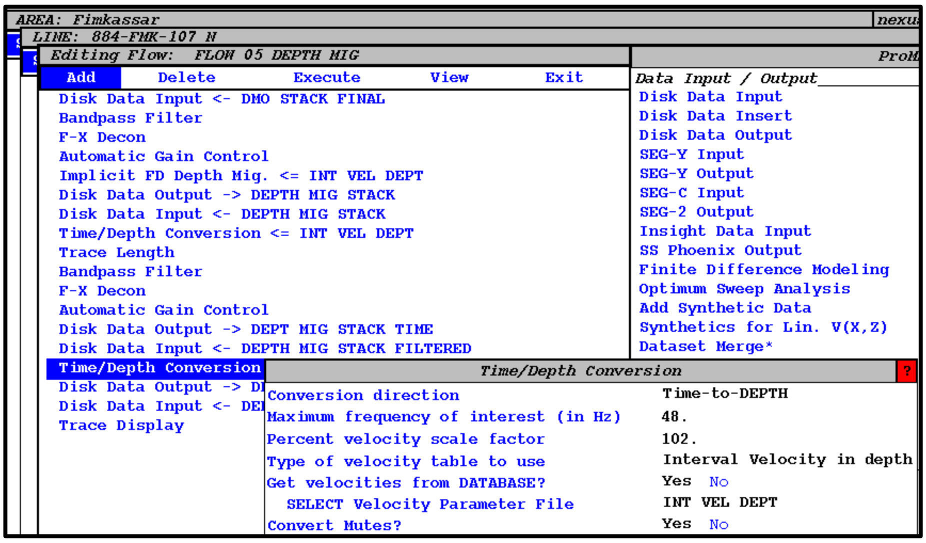

Figure 5.26 flow for time to depth conversion after processing

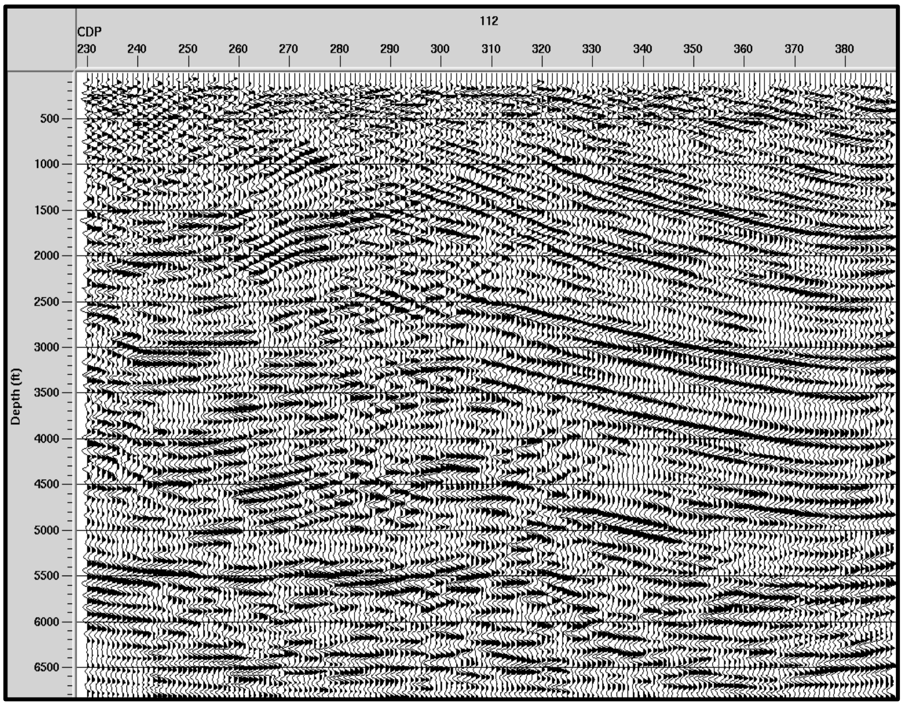

Figure 5.27 Final depth migrated stack884-FMK-107

5.3.4 Interpretation on Depth Migrated Stack

The Final stage of work will be again doing interpretation on depth migrated stack. As shown in figure 5.28 reflectors are more prominent than on time section and specially the resolution of horizons and faults in second sheet is more visible. The well data also matches and validates the depth of horizons marked on section and those in Formation tops.

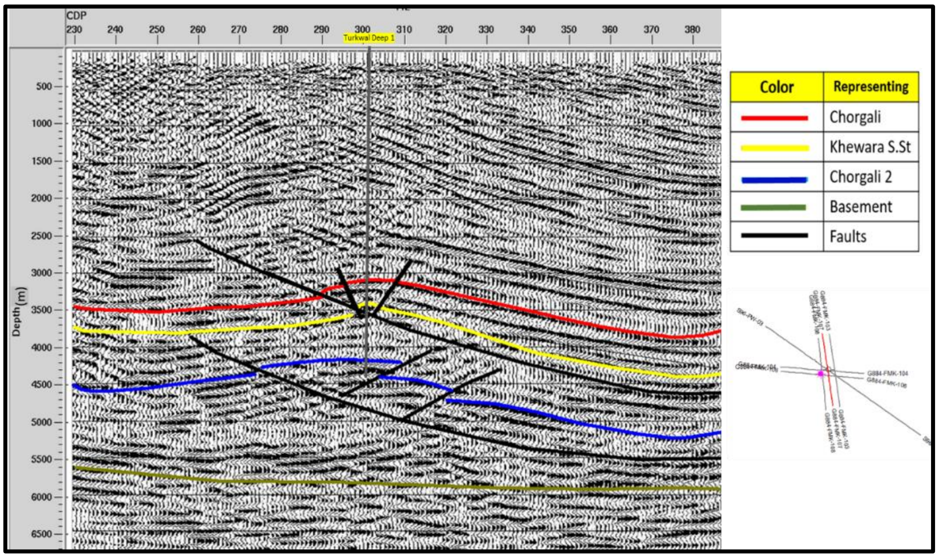

Fig 5.29 Final depth migrated stack 884-FMK-107 with interpretation

CONCLUSIONS

The following conclusions are drawn from the work done in this thesis:

1. Presence of reverse (Thrust) faults indicates that Fimkassar area lies in compressional regime. Seismic data interpretation shows that Fimkassar oil field has triangular zone structure formed by major thrust that is dipping in the NW direction while the back thrust that is dipping in SE direction.
2. Time and Depth contour maps of Eocene and Paleocene Formations help us to confirm the presence of anticlinal structure/positive geometry in the area.
3. Velocity modelling helped in understanding the velocity variations in the subsurface and geological anomalies present in the area.
4. Post Stack migration helped in understanding more accurate/true subsurface image by enhancing the reflectors and faults which resulted in more confident interpretation.

REFERENCES

Aamir, M., & Siddiqui, M. M. (2006). Interpretation and visualization of thrust sheets in a triangle zone in eastern Potwar, Pakistan. *The Leading Edge*, *25*(1), 24-37.

Butler, R. W., & Prior, D. J. (1988). Tectonic controls on the uplift of the Nanga Parbat Massif, Pakistan Himalayas. *Nature*, *333*(6170), 247-250.

Coward, M. P., Rex, D. C., Khan, M. A., Windley, B. F., Broughton, R. D., Luff, I. W., ... & Pudsey, C. J. (1986). Collision tectonics in the NW Himalayas. *Geological Society, London, Special Publications*, *19*(1), 203-219

Coward, M. P., & Potts, G. J. (1983). Complex strain patterns developed at the frontal and lateral tips to shear zones and thrust zones. *Journal of Structural geology*, *5*(3-4), 383-399.

Karslı, H., & Dondurur, D. (2018). A mean-based filter to remove power line harmonic noise from seismic reflection data. *Journal of Applied Geophysics*, *153*, 90-99.

Erohina, T., Cooper, A., Handwerger, D., & Dunbar, R. (2004). Seismic stratigraphic correlations between ODP Sites 742 and 1166: implications for depositional paleoenvironments in Prydz Bay, Antarctica. *COOPER, AK, O'BRIEN, PE & SHIPBOARD SCIENTIFIC PARTY. Prydz Bay–Cooperation Sea, Antarctica: Glacial History and Paleoceanography Sites*, 1165-1167.

Gee, E. R., & Gee, D. G. (1989). Overview of the geology and structure of the Salt Range, with observations on related areas of northern Pakistan. *Geological Society of America special paper*, *232*, 95-112.

Iqbal, M., & Helmcke, D. (2004). Geological interpretation of earthquakes data of Zindapir Anticlinorium, Sulaiman foldbelt, Pakistan. *Pakistan journal of Hydrocarbon Research*, *14*, 41-47.

Kazmi, A. H., & Rana, R. A. (1982). Tectonic map of Pakistan Geol. *Surv (Pakistan) Quetta*, *39*, 283-300.

Khan, S. H. (1990). James W. McDougall 1 Department of Geology, Oregon State University, Corvallis.

Khan, K. A., & Akhter, G. (2011). Workflow shown to develop useful seismic velocity models. *Oil and Gas Journal*, *109*(16), 52-61.

Morey, S. L., Baig, S., Bourassa, M. A., Dukhovskoy, D. S., & O'Brien, J. J. (2006). Remote forcing contribution to storm-induced sea level rise during Hurricane Dennis. *Geophysical Research Letters*, *33*(19).

Moghal, M. A., Saqi, M. I., Hameed, A., & Bugti, M. N. (2007). Subsurface geometry of Potwar sub-basin in relation to structuration and entrapment. *Pakistan Journal of Hydrocarbon Research*, *17*, 61-72.

Qadri, S. T., Islam, M. A., & Shalaby, M. R. (2019). Application of well log analysis to estimate the petrophysical parameters and evaluate the reservoir quality of the Lower Goru Formation, Lower Indus Basin, Pakistan. *Geomechanics and Geophysics for Geo-Energy and Geo-Resources*, *5*(3), 271-288.

Stumpf, R. P., & Pennock, J. R. (1989). Calibration of a general optical equation for remote sensing of suspended sediments in a moderately turbid estuary. *Journal of Geophysical Research: Oceans*, *94*(C10), 14363-14371.

Shah, S. M. I. (2009). Stratigraphy of Pakistan: GSP memoir 22. *Geological Survey of Pakistan, Quetta*.

Treitel, S., 1974, The Complex Weiner Filter: Geophysics, 39-2, 169-173.

Uygun, O. E. (2016). *Comparison of different seismic filtering techniques on prestack inversion for Penobscot Area-Nova Scotia* (Doctoral dissertation, Michigan Technological University).

COMPLEX VELOCITY MODEL BUILDING OF FIMKASSAR AREA, UPPER INDUS BASIN PAKISTAN

by Muhammad Muneeb

Submission date: 09-Sep-2021 01:44PM (UTC+0500)
Submission ID: 1644367833
File name: THESIS_DRAFT_MS_PLAGRISM_CHECK_Muneeb_Final.pdf (363.83K)
Word count: 8408
Character count: 42637

COMPLEX VELOCITY MODEL BUILDING OF FIMKASSAR AREA, UPPER INDUS BASIN PAKISTAN

ORIGINALITY REPORT

6%	5%	2%	4%
SIMILARITY INDEX	INTERNET SOURCES	PUBLICATIONS	STUDENT PAPERS

PRIMARY SOURCES

1	www.slideshare.net Internet Source	1 %
2	seg.org Internet Source	1 %
3	Submitted to Curtin University of Technology Student Paper	1 %
4	Submitted to Higher Education Commission Pakistan Student Paper	1 %
5	academic-master.com Internet Source	1 %
6	lra.le.ac.uk Internet Source	<1 %
7	glossary.oilfield.slb.com Internet Source	<1 %
8	documents.mx Internet Source	<1 %

www.cambridge.org

9 Internet Source <1%

10 Stephen J. Hill, Andreas Rüger. "Illustrated Seismic Processing Volume 1: Imaging", Society of Exploration Geophysicists, 2019 <1%
Publication

11 Perveiz Khalid, Qamar Yasin, Gmd Sohail, Jam Muhammad Kashif. "Integrating core and wireline log data to evaluate porosity of Jurassic formations of Injra-1 and Nuryal-2 wells, Western Potwar, Pakistan", Journal of the Geological Society of India, 2015 <1%
Publication

12 Ravikant, V.. "Zircon U-Pb and Hf isotopic constraints on petrogenesis of the Cretaceous-Tertiary granites in eastern Karakoram and Ladakh, India", LITHOS, 200906 <1%
Publication

13 Derman Dondurur. "Velocity Analysis", Elsevier BV, 2018 <1%
Publication

14 M. Giustiniani. "Characterization of the shallow aquifers by high-resolution seismic data", Geophysical Prospecting, 5/9/2008 <1%
Publication